INVESTIGATION OF EROSION WEAR IN SLURRY PIPE BEND USING CFD

A

THESIS

Submitted in partial fulfillment of requirements for the award of degree of

Master of Engineering (M.E)

In

Thermal Engineering

Submitted by

PRINCE KUMAR

(Roll No. 851283004)

Under the guidance of

Dr. SATISH KUMAR

Assistant Professor, MED

Thapar University, Patiala

MECHANICAL ENGINEERING DEPARTMENT

THAPAR UNIVERSITY, PATIALA – 147004

JULY 2015

CERTIFICATION

I, Prince kumar, declare that this thesis report entitled "***Investigation of erosion wear in slurry pipe bend using CFD***", submitted towards fulfillment of the requirements for the award of Master's Degree in Thermal Engineering, in Mechanical Engineering Department of Thapar University, Patiala, is entirely my own work. This document has not been submitted for any degree in any other institution.

Date: 14/7/15
Place: TU, Patiala.

Prince kumar
851283004

Thapar University, Patiala

This is to certify that above statement made by the candidate is correct and true to the best of my knowledge.

Dr. Satish Kumar
Assistant Professor, MED
Thapar University, Patiala

Countersigned by

Dr. S.K. Mohapatra
Senior Professor and Head
Mechanical Engineering Department
Thapar University, Patiala

Dr. S.S. Bhatia
Dean
Academic Affairs
Thapar University, Patiala

ACKNOWLEDGEMENT

First of all, I would like to express my gratitude to Dr. S.K Mohapatra, Senior Professor and Head of the Mechanical Engineering Department, Thapar University, Patiala for his patience guidance and support throughout this report. I am truly very fortunate to have the opportunity to work with him. I found his guidance to be extremely valuable.

I also express my special thanks to Dr. Satish Kumar, Assistant Professor and PG. coordinator, providing me opportunity to conduct this work and bring it out in present from.

Last but not the least; I want to convey my heartiest gratitude to my parents and my friends for their immeasurable lobe, support and encouragement.

Prince kumar

Prince kumar

ABSTRACT

Erosion wear is the serious/major problem in industrial, power plants utilities like pipe-line, bends, tees, impellers and pump due to impingement of solid particulates at high velocity entraining through fluid. Hence erosion wear shorten the life of the concerned components and an extra expenditure for the maintenance and repair. In thermal power plants large amount of fly ash and bottom ash is produced from the pulverized coal –fired in boiler. The fly ash is collected in ESP while the bottom ash transported to ash-pond in the slurry form through pipe-line system leads to erosion wear in the pipe line. Many authors and researchers have reported that erosion rate is affected by various parameters like solid concentration, velocity, impact angle, particle size, target material etc.

In the present study, the erosion wear in the pipe-bend for the flow of solid-liquid is evaluated in the CFD code FLUENT. Also the effects of velocity, solid concentration and particles size have been studied numerically by varying these parameters from ranges of 0.5m/s to 2.5 m/s, 2.5% to 10% and 162μm & 300μm respectively. The k-ε turbulence model for fluid flow and discrete phase to track the solid particles in the flow field are used in simulation. The magnitude and location of the erosion rate are influenced by prescribed conditions. The results show a good agreement with the previous work of many researchers and authors.

CONTENTS

LIST OF FIGURES

LIST OF TABLES

NOMENCLATURE

A_{face}	Cell face area at the wall
a_x	Maximum packing limit.
a_l	Volume fraction of liquid phase
a_q	Volume fraction of solid phase
C_D	Drag coefficient
d_p	Diameter of particle
e_{ss}	Coefficient of restitutions
$f(\alpha)$	Angular function
$g_{o,ss}$	Distribution function
K_{ls}	Liquid solid exchange coeeficient
Re	Reynolds number
$R_{erosion}$	Erosion rate
v_f	Fluid velocity
v_l	Velocity of liquid phase
V_l	Volume of liquid phase
v_p	Relative particle velocity
v_q	Velocity of solid phase
V_q	Volume of solid phase

α	Impact angle
ρ_l	Density of liquid phase
ρ_q	Physical Density of solid phase
μ_{col}	Collisional viscosity
μ_s	Shear viscosity of solid
μ_f	Molecular of viscosity of fluid
μ_s, fr	Frictional viscosity
μ_s, kin	kinetic viscosity
$\bar{\bar{\tau}}_l$	phase stress tensor for liquid
$\bar{\bar{\tau}}_s$	phase stress tensor for solid
λ_q	Bulk viscosity of solid

φ	Internal friction angle
θ_s	Granular temperature
∇p_s	Solid collisional stress

CHAPTER 1 INTRODUCTION

Many engineering industries and plants like thermal power plant, cement plant are comprise of erosion wear due to transportation solid-liquid mixture and solid-gas through pipe-line system. In thermal power plants large amount of ash (fly and bottom) is generated from coal used as a fuel for generating electricity. This collected ash in hoppers is transported through components like pipe-bend, plugged tees, tubes, valves, elbows and centrifugal slurry pump etc. to ash pond in the form of slurry (water and ash) having very large amount of abrasive and quartz in it Modi et al. (2000). Hence the pipe-line system suffers from erosion wear damage due these abrasive's impact angle and velocity.

Many authors have been found erosion wear in pipeline system of production, transportation of petroleum products Edward et al. (2001), oil and gas production (Bozzini et al. (2003), Chen et al. (2004), Shah et al. (2007), Zhang et al. (2007), Okita et al. (2012)), production of oil Gnanuvela et al. (2009), erosion wear in boilers, space craft, pipe line, turbines and coal processing system Mazumder et al. (2012).

Erosion wear takes place more severe in curved surface than straight section (Shah et al. (2007), Stack et al. (2011)). An example from one of the above stated components is pipe-bend or elbow which is connected in the pipe line system. The main function of the bend is to give the horizontal, vertical and inclined turn to the transporting fluid/mixture inside it.

Many researchers have proposed many experimental and theoretical erosion models and expressions to evaluate the magnitude and location of solid-liquid erosion wear of the system. In the present study erosion wear is investigated in the pipe-bend using the CFD.

1.1 EROSION WEAR

Erosion wear is a phenomenon in which material removed from the target surface by impacting solid particles at high velocity. The erosion generally occurs in channels, pipe- bends, valves, fitting components etc. These solid particles are directed by pumps and compressors in hydraulic and pneumatic system respectively industrial utilities, thermal power plants etc. Erosion is cause of failure of the parts,

unpredictable damages; shorten the life of concerned parts or system. Hence the erosion leads to extra expenditure for the eroded parts. Examples**:** Transportation of slurry in pipe-line system at thermal power plants. Pneumatic conveying of ash in power stations, cement plants and other sectors.

1.2 WEAR

Wear is defined as the removal of material between the sliding surfaces due to interlocking or roughness on the surfaces. Wear tends to loss of the durability and reliability of the subjected parts. So the proper investigation and care must be taken to control it in the emerging technology.

1.3 TYPES OF WEAR

The various types of wear are exist nature due to relative motion between the sliding surface, matters, bodies and in the mixture of physical matters solid, liquid and gas. Types of wear are given below.

a) Abrasive Wear

In abrasive wear a hard material is moved over the material, an interlocking is formed between these causing a plowing action formed. Due to plowing action the material from soft material surface is plastically deformed or removed away and a groove is formed on the eroded material surface as shown in figure 1.1. Example of abrasive wear is: shovels on the earth moving machinery.

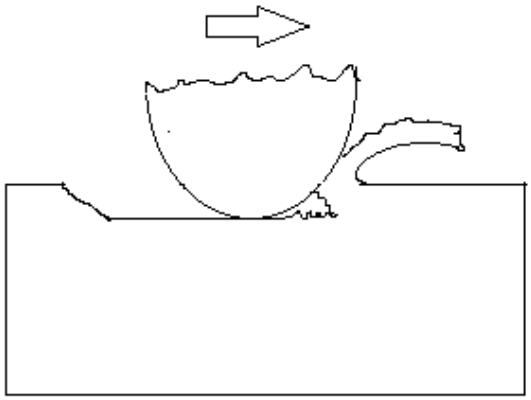

Figure 1.1: Abrasive Wear

b) Adhesive Wear

In this type of wear the contacting interfaces have enough adhesive/bonding strength to resist the relative motion between these. A dislocation or a crack is initiated at the mating zone under the tensile and shearing action due to this bonding strength.

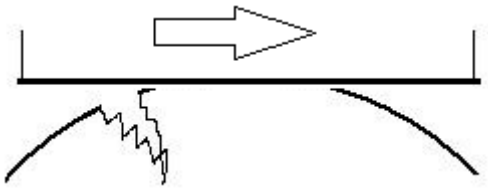

Figure 1.2: Adhesive Wear

c) Corrosive Wear

In corrosive liquid and gas flow products are formed on the surface between sliding surfaces due to chemical and electrochemical reactions. A bulk wear phenomenon is formed at the surface if the products sticks strongly on the wall/surface and treats as a bulk material. Some time products may not treat like bulk solids but products leads to wear due to reactions between solids and corrosive fluid.

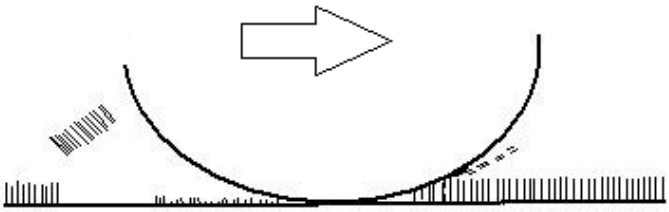

Figure 1.3: Corrosive Wear

d) Fatigue wear

The fatigue wear exist when the surfaces are subjected to large repetition or opposite moving under the local stress and generates the solid-particles which lead to wear between the surfaces e.g. rolling contacts (ball bearing). Low-fatigue and High fatigue are the types of fatigue wear, depends upon the number of contacting cycles.

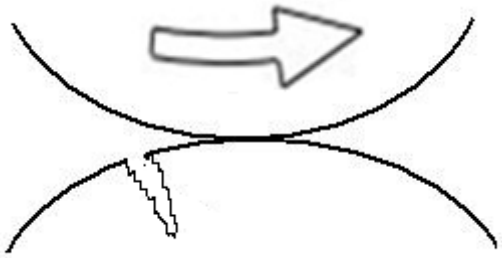

Figure 1.4: Fatigue Wear

1.4 MECHANISM OF EROSION WEAR

In erosion wear phenomenon, the solid particles forcefully entrained in carrier fluids (liquids and gases) by pump and compressors to pipe-line where these solid particles strike at the wall of system. At the same time little amount of material is eroded away from the surface/target body due to high velocity impact of solid-particles. It is generally found in industrial processes, power stations and in many other areas while transporting the solid-liquid and gas-solid mixture through the pipe line system. The subjected components to erosion wear are pipelines, bends, elbows, tees, plates, slurry-pumps etc. The durability and reliability of these components decrease due to erosion wear. Also erosion wear is a cause of damaging of parts and extra expenditure for the maintenance, replenishment of damaged components/parts. Classifications of erosion wear are:

- Extrusion and forging
- Plowing
- Subsurface deformation and cracking.

1.5 TYPES OF EROSION WEAR

Several types of erosion wear are described below:

a) Cavitation erosion

In this type of erosion wear the gas bubbles are formed in the flow field due to low pressure than saturated pressure of the liquid. The formed bubbles make bombardment on the wall and tend to erosion wear at the particular impacting region. Cavitation in slurry transportation is an example of cavitation erosion wear.

b) Jet erosion

It is a process in which solid- liquid mixture strikes in the form of jet with high velocity and at an angle on the stationary wall. Due to the impact of the jet small amount of material is removed from target surface. W and U shape erosion profile is formed on the target surface in liquid and gas in jet impingement respectively Masouri et al. (2014).

c) Liquid drop erosion

Due to the impingement of liquid drops at the surface, the material is gradually removed from the impacting zone of the surface.

d) Particle erosion

It is also a wear mode, in which repetition impact of solid particles exist as a result, loss of material from the impacting zone. The particles accelerate and de-accelerate when flow through liquid or gas. The direction of the solid particles may deviate in the carrier fluids. Solid particles erosion used in sand blasting and high- speed abrasive water jet cutting Patnaik et al. (2010).

e) Slurry erosion

In this type of erosion the fine solid particles flowing through liquid impacts over the wall of domain with high velocity. The kinetic energy and impact energy of the mixture increased due to increasing the density and mass of eroding particle which results in removal of small amount material from impacting zone of the surface.

1.6 PARAMETERS AFFECTING THE EROSION WEAR

There are several parameters affecting the erosion wear rate have been listed below:

a) Abrasive properties

- Concentration of slurry
- Particle size
- Hardness of erodent
- Yield strength
- Particle shape

b) Type of contact

- Impingement and Impact angle
- Sliding or Rolling
- Potential of hydrogen (pH)
- Carrying fluid - dry/wet
- Temperature
- Impact speed of erodent
- Impact force of erodent

c) Target materials properties

- Corrosion resistance
- Ductility
- Elastic modulus
- Fracture toughness
- Hardness
- Microstructure Toughness
- Work-hardening characteristics

1.7 SLURRY FLOW

The mixture of solid particulates and liquid is known as slurry, which in transported in pipeline system in chemical, coal, food, minerals, oil production, thermal power stations and many other industries. The common examples of slurry are: sand-water slurry, ash-water slurry, coal-water slurry, coal-oil slurry etc. The slurry flow is also known as multiphase, in which the velocity of the solid particles should be enough to maintain it in suspended form. The single phase flow is known as homogeneous flow at all velocity of flow, while the slurry flow behaves as heterogeneous and homogeneous depends upon the solid concentration in it.

Large numbers of parameters which contribute to change the flow behaviour of the slurry are conduit orientation/dimension, particle size distribution (PSD), particle shape, particle density, solid concentration, flow velocity etc.

Classification of slurry:

- **Settling slurry**

  Non-uniform and coarse particles of solid in the solid-liquid mixture form heterogeneous type of slurry. In this type of slurry the heavier and coarse particles settle-down at the pipe-line wall and light or small size particles suspended in the carrier fluid as shown in Figure 1.5.The settling of the slurry also depends upon the velocity of the mixture.

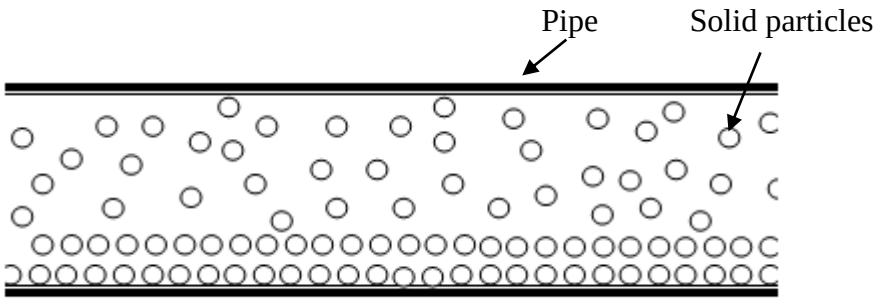

Figure 1.5: Settling slurry in pipe-line

- **Non-Settling slurry**

  In non- settling slurry the present solid particles are very fine in nature and uniformly distributed in the flowing region which form a homogenous mixture as shown in Figure 1.6. However the slurry behaves like a viscous in manners along with non-Newtonian characteristics.

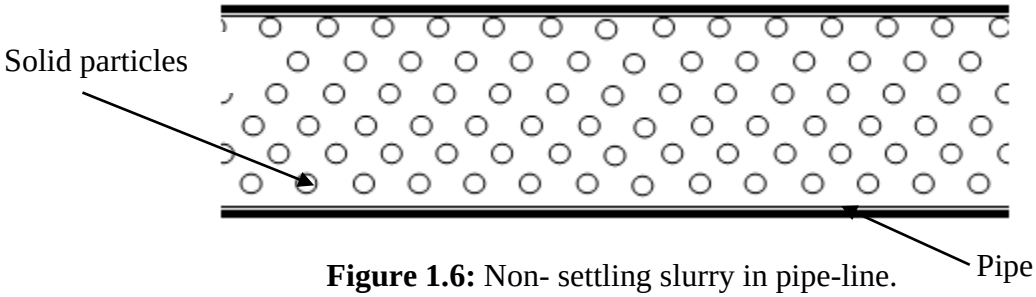

Figure 1.6: Non- settling slurry in pipe-line.

1.8 EROSION TEST RIGS

The devices which are used to evaluate the erosion wear rate of the test samples in terms of mass loss. The prepared test sample rotates along the spindle and submerged

in the slurry pot. Due to high speed of the test sample against the slurry impacts over the surface at an angle and material from the impingement zone is removed away due to particles impingent over it. Finally the weight loss is calculated to define the erosion rate. Several types of erosion test rigs are used by researchers. Each of the erosion test rig have different characteristics and field conditions but erosion mechanism is same. Types of test rigs are discussed here:

a) Concentric cylinder test rig

This type of tester is used when the difference between the density of liquid and density liquid is less as the particles may settle down during the wear test.

b) Falling jet test apparatus

The specimens rotated in the vacuum chamber and jet of solid-liquid mixtures falls on the test specimen under the gravity action.

c) Coriolis erosion tester

This tester is used to evaluate the erosion wear resistance on different target materials under the low interaction intensity conditions (low velocity and low impact angle) of solid particles.

d) Jet in silt apparatus

The slurry erosion tester is used to evaluate the erosion wear of different type of coated materials. The tester consists of a transparent tank holding two compartments upper but smaller in diameter and lower compartment bigger in diameter store the liquid. In the upper tank, the fresh water is circulated by the pump to the test section. The four samples in test section are fixed which are subjected to uniform upward flow water and the rest water is goes to lower tank. The liquid jet from the nozzles is set at the centre of the test sample and the slurry is sucked and impinges on the test sample at high velocity leads to loss of material from the target surface.

e) Pot tester

The tester is used to evaluate the erosion wear of the rotating test sample after interval of the time at different concentrations. It consists of pot carrying slurry in which sample specimens are rotated at specified rpm. After interval of time the erosion rate is measure in the form of weight loss of the test sample.

1.9 MOTIVATION OF THE PRESENT WORK

Evaluation erosion wear of material due to flow of (solid-liquid/gas-solid) is very typical task. Large numbers of parameters are present which influence the erosion wear. For example impact velocity, impact angle, particle size, target material and concentration of solid phase etc. The theoretical existing erosion models may or may not be able to find the erosion wear of the material at all the conditions. So the motivation of the present work is to numerically investigation of erosion wear for the flow of solid liquid in pipe bend. Also to analyze the effects of velocity, solid concentration and particle size on erosion wear due to transportation of multiphase flow (bottom ash-water) using discrete phase model (multiphase model) in Computational fluid dynamics code FLUENT by varying the above stated parameters.

Computational fluid dynamic is a useful tool to predict the internal fluid behavior (single and multiphase flow), distributions of flow field, particle motion and erosion wear rate graphically and numerically of any complex geometries. In the CFD without any experimentation on protocol and models, the approximate results are evaluated with the physical conditions and models. Due to such enhanced advantages of the CFD now days widely used in industrial purposes and research areas.

CHAPTER 2 LITERATURE REVIEW

In the literature review the study on erosion wear by many authors have been discussed. This chapter has been made after the complete study of their research papers to describe their investigation, findings, output, and results for the erosion wear. The numerical and experimental methodology was used by the researchers to evaluate of erosion wear due to transportation of the solid particulates through hydraulic and pneumatic system.

Modi et al. (2000) performed the Jet impingement test on the 304 stainless steel specimen with coal and bottom ash slurry to evaluate the erosion wear. The high erosion wear was found with bottom ash slurry due to presence of the carbon, un-burnt coal and α particles in the bottom ash. They observed that the coal particles breakdown into small particles due to collision with wall and may not have enough energy to deform the target wall surface, hence less erosion rate was found with coal slurry. Also the results revealed that the high weight loss in the initial stage and became stable in the final stage along the travel distance of both the slurries.

Zhang et al. (2000) performed simulation for the solid-liquid two phase flow to evaluate the erosion-corrosion in the pipe in CFD. The k-ε turbulent model and Lagrangian-model were used with the boundary conditions velocity inlet and outlet over the domain. The glass material of particles size 8μm was used as erodent material. The results obtained for the erosion rate, corrosion were found good agreement with experimental results of Nesic & Postlehwaite.

Edward et al. (2001) numerically studied the solid particle erosion in Standard elbows, long radius elbows and plugged tees. The**y** found more momentum transfer in long radius elbow instead of standard elbow. Due to the momentum the particles does not strike to the wall. The large amount of particles followed the fluid streamline or remain suspended in the fluid through the long curvature (don't strikes early to the wall). The gradual redirection of the flow leads to less erosion than instantly flow redirection. They observed the particles lose the velocity near the stagnant zone due to fluid cushion effect due this particles don't strikes the wall and low erosion wear was observed in plugged tees. Also they found low erosion depth in long radius elbow instead of standard elbow and plugged tees.

Bozzini et al. (2003) studied erosion phenomenon of pipe bend in CFD code Fluent by using four phases (oil, sea water, hydrocarbon mixture and sand particles). The Discrete Phase Model was used to track solid particles of diameter 300 μm. They observed the solid particles have less transporting capacity at low velocity and settle-down pipe-bend where the erosion wear was examined at the same time they increased the gas volume flow rate in the mixture to improve the erosion rate. The total mass flow rate of particles was affecting the fluid flow behaviour not the erosion rate. The high velocity of mixture had generated high drag force and inertia force on solid particles which push the solid particles toward outer radius of bend where the high erosion rate was examined.

Wood et al. (2003) performed CFD simulation to evaluate the erosion induced by sand water in steel pipe-bend of pilot and laboratory scaled. The particle tracking and turbulence models were employed in the simulation process. The almost constant velocity as well as small impact angle was observed in straight pipe but fluctuated velocity profile and high impact angle were obtained in the bend cross-section. Due to this high velocity and impact angle the high erosion rate was found in the bend zone than the straight pipe. The experimental and numerical results had found good agreement.

Chen et al. (2004) studied erosion wear on 1 inch elbow and plugged tee of aluminum in CFD code CFX code by considering air and sand particles (150μm in diameter). Grid independent test and particle independent test had been carried out for both the geometries. In lagrangian model, two wall collision approaches (Stochastic rebound and Forder rebound) were used to evaluate the erosion rate at different velocities (15.24m/s, 30.38m/s, 45.72m/s). The results obtained with Forder rebound model had 15% more erosion rate in elbow and large number of re-circulations leads to local erosion rate in tee domain. But stochastic rebound model's results have made a good agreement with experimental results. Finally, the average erosion wear location was found by graphical approach for the elbow and tee.

Habbib et al. (2004) numerically investigated the erosion rate at different contraction ratio of carbon steel straight pipe. The simulation was carried out at different velocities, different particles sizes for the contraction ratio of the upward and down ward of pipe. The high erosion rate was found at contracted zone with different

particles size at constant velocity for the upstream and downstream pipe. Also thrice erosion rate was examined with double size particles in up and downstream at different velocity at the same zone.

Wood et al. (2004) studied slurry erosion rates in horizontal pipe-bend using CFD code-Fluent V5.4. The results were predicted at midway of the straight pipe and 45^{o} along the bend. The particle velocity and supply of particles were varying along with the peripheral angles. The erosion rates, sand volume, impact angle, impact velocity, were predicted for the straight pipe and bend. Negative impact angle or reverse flow were found at 90^{o} and 270^{o} plane angles of pipe-bend. Due to the particles loading and impact velocity of the particles, somewhat erosion wear was examined at these angles and resulting the damaging of material at the particular zone.

Gnanavelu et al. (2009) predicted wear rate of material due to erosion by jet impingement tester method in CFD code FLUENT. With particle tracking scheme the simulations results were validated with experimental data at different impingement angles in two cases (90^{o} and 105^{o}, 135^{o}). At jet impingement angle of 90^{o} with velocity 7m/s three different erosion scars were predicted on target wall. The particles were impacting near the centerline at stagnation point with low velocity due to high pressure. Away from the centre the particles velocity was high where the high erosion was examined. At impingement angle of 105^{o} at 5m/s asymmetry erosion profile was found and also the unequal number of particles were impacting at each side of stagnation point. But at 135^{o} angle, the particles were impacting at a single side of stagnation point. They observed difficulties to maintain the distance between nozzle and test surface, particles-particles collisions and the size and distribution of particles at different angles except normal angle of test specimen.

Graham et al. (2009) investigated slurry erosion in the pipe bend and cross-cylinder extended in pipe by experimental and numerical approaches. the surface condition for the slurry flow regions was checked with coordinate measuring machine and 3D laser scanner and compared CFD results with experimental data and paint modeling. They observed maximum erosion rate at the exit of the elbow-pipe wall, at top surface of cylinder and at vicinity (around the cylinder) of the complex domain. At the top surface of the pipe the results were deviating from the experimental results. The

predicted results by Finnie and Grant and Tabakoff erosion models were found agreement with the experimental results.

Gnanuvela et al. (2011) investigated slurry erosion rate over a 90^o flat plate using Jet impingement tester. They predicted the erosion ratio with experimental setup and three models in numerical approach at velocities 5m/s and 10 m/s. A good agreement between Huang erosion model and experimental results was found than Combined Finnie and Bitter erosion model. The erosion ratio was found due to deformation mechanism at impact angle from 80^o to 30^o and then deviated type erosion ratio was observed with cutting mechanism up-to impact angle ($\leq 30^o$).

Stack et al. (2011) studied the erosion-corrosion phenomenon using CFD-code over the Fe pipe-bend at different mass flow rate of solid particles and at different volume fraction. They observed that with increasing the solid concentration in the slurry the bend section was greatly influenced by the erosion wear than the straight section (pipe) but at the same time erosion dissolution (corrosion) was decreased at the particular region or erosion enhance corrosion.

Zhang et al. (2011) numerically investigated the maximum erosion damage and location in the elbow and also studied the effect of slurry velocity, bend orientation and angle of the elbow. The discrete element method was used in the simulation process to track and identify the interaction between the wall and solid particles. They observed low porosity, high drag force, and high relative velocity (due to friction between particles) at the high concentrated zone. The maximum erosion was found at 25^o of the elbow and different magnitude of erosion wear was also obtained at different slurry velocities (6m/s, 9m/s, 18m/s and 36 m/s). The impact force was observed linear up to slurry velocity 9m/s and faster as well as non-linear beyond 9m/s up-to 36m/s. they also observed the gravitational force reduces the bouncing tendency of the particles. The erosion wear was found near the outer wall of the elbow.

Mazumder et al. (2012) studied the effect of liquid and gas velocities on magnitude and location of maximum erosion in U- bend. They obtained that the maximum erosion location away from inlet of bend in gas-solid flow while at near for the liquid-solid flow with small particles and low velocity. Same location was found with

100μm particles at high velocities for both the flow (liquid and gas)-solid. Also results revealed that maximum erosion at same location with all size of particles for solid- liquid flow and only with larger particles in gas-solid flow.

Njobuenwu et al. (2012) evaluated the erosion wear on cross duct 90^o bend of four different sizes. The primary and secondary erosion was predicted in the simulation and compared with the five different erosion models, experimental data and found good agreement with the erosion models. The maximum and primary erosion was predicted on the concave wall near the entrance of bend then on the convex wall. The observed erosion wear was dependent on the momentum, velocity of the particles and number of particles tracked at the point of collision on the wall. A weak secondary erosion depth was also found at the concave wall near the exit of bend after collision of particles from the convex wall. In contrast all the physics of the erosion magnitude and location in the bend were the function of the restitution coefficients of the particles.

Okita at al. (2012) studied the effects of air-water fluid viscosities and particles size on the erosion rate of flat plate by positioning at different angles. They observed the erosion ratio was decreased by increasing the viscosity of fluid in a mixture of *sand-water* contained particles size 20µm and 150 µm. the erosion ratio was decreased significantly with small size particles at high viscosity. But same erosion ration was found with 300µm particles at all viscosities. They found high axial velocity near the centerline and laminar type flow at exit of nozzle with viscosity of fluid 100cP and 120µm sand particles. While low velocity and turbulent type flow were found in 1Cp at same zones. The velocity was found low due to high pressure at stagnation point and increasing radially outward from centerline which tends to erosion. *In air-solid*, the erosion ratio was predicted at different impact angles, at two different shape and size (150 µm, 300 µm) of sand particles. High erosion ratio was found with 150 µm particles at all velocities and small impacting angles. The comparison was made between Oka, E/ECR equations and experimental data. The obtained results for erosion wear were steeper in air-solid flow than solid- liquid flow.

WU et al. (2013) evaluated the erosion in oil pipe lines of different sections with 0.5% sand contamination. The less erosion rate was observed at inner side of straight pipe near the bend due to secondary flow and high erosion was found at the extrados

of the bend. The erosion rate was also increasing with impact angle of the sand particles. The results revealed that erosion ratio was decreased at 30^o bend instead of 45^o and 90^o bend, by decreasing camber angle. In long radius bend low secondary flow was examined and low erosion was observed. Also erosion was found with expansion of pipe sections, in which recirculation is decreased and leads to less erosion.

Hadziahmetovic et al. (2014) predicted the erosion due to pneumatic conveying in elbow with CFD. After grid independent and particles independent test the results were revealed for the erosion depth and velocity at different planes in the elbow. The obtained results with Stochastic rebound model were more accurate than deterministic rebound models. The maximum erosion was found at 46^o along the elbow curvature.

Masouri et al.[2014] predicted erosion rate with two methodologies i.e. air –sand and water-sand using CFD code. Particles tracking approach was used to evaluate the erosion rate at different angles and different velocities for both the cases. The parallel flow path of particles in air and equal normal impingement and impact angles were found in air-solid erosion mechanism. But deviated-type flow path of particles and unequal angles were found in solid-liquid erosion. In air- solid flow, erosion depth (U-shape profile) was proportional to impact frequency of air, velocity and incident angle of impacting particles. In solid-liquid flow, near the target wall and at center of injection low velocity (due to static pressure) was observed which leads to a stagnation point where erosion depth decreases. Away from centre of injection along radius, the velocity was increasing which leads to high erosion depth and formed a W-shape erosion profile on wall.

Pereira et al. (2014) studied for the erosion due to particles in elbow using Euler-lagrange approach in CFD-UNSKYFL3D code**.** The experimental results of **Chen et al. (2004)** were compared with four computational erosion relations given by (Alhert et al. (1994), Neilson and Gilchrist et al. (1968), Oka et al. (2005), Zhang et al. (2007)). Similar flow behaviour and different magnitudes of erosion were obtained in all the four erosion models. The results obtained with Oka and Zhang erosion models were good agreement the experimental results. They observed a noisier type penetration ratio with less number of particles and an effective penetration ratio was

formed with 50,000 particles only in Oka erosion model. The erosion penetration was influenced by surface roughness and friction factor.

Safaei et al. (2014) investigated the erosion wear on 90^{o} bend with micro and nano meter copper particles using discrete phase erosion model. Initially they validated the erosion model with Chen et al. (2003). The effect of the velocities and six different particles size were examined at different solid concentrations. The maximum erosion rate obtained with micro size particles was many times more than nano size particles at high velocity. Also the effect of high concentration was examined and high erosion rate was found with increasing the solid concentration. The graphical representation was made for the threshold impact velocity and threshold particles size. threshold velocity means below which negligible erosion rate was found.

Zeng et al. (2014) studied the erosion-corrosion on carbon steel elbow using CFD codes Gambit/Fluent. The mesh interval size was 0.004 m and turbulent flow model was employed. The simulations were carried out using Single phase, DPM, Euler models for pure erosion rate, pure corrosion rate, erosion–enhanced corrosion rate and corrosion–enhanced erosion rate. Due to gravitational effect, the sand concentration was found high at inner side of upstream straight pipe and also high erosion magnitude was observed at the same zone. Erosion magnitude and sand concentration were shifting from inner to outer wall along the elbow curve. The erosion rate was increasing along the outer radius (at azimuth angles 130 ^{o}, 180 ^{o} and 230^{o}) and decreasing along the inner radius (at azimuth angles 0^{o}, 50^{o} and 310^{o}) of elbow. At downstream pipe-section the erosion magnitude at outer wall was found contrary to upstream pipe. Due to the different hydrodynamics effects (high inertia force, drag force and secondary flow) on solid particles, the particles were deviating from the streamline of liquid and impacting on the outer wall of elbow at high kinetic energy with high frequency. Thus the high sand concentration was found at outer walls of elbow and downstream pipe. Finally the erosion rate, sand concentration, secondary flow were shown by contours at different sections of elbow

Chen et al. (2015) predicted the erosion of liquid-solid flow in three different bend angles with CFD-DEM. In simulation the maximum erosion was found near the exit of the all bends and minimum erosion rate was found in smaller bend angles. The predicted results agreed the experimental results.

CHAPTER 3 MULTIPHASE MODELING FOR EROSION RATE

Computational fluid dynamics (CFD) is an important tool which is used to solve the problems associated with fluid flow, heat flow and some reactions by simulating in computer. The CFD solve the problem by various numerical approaches and by algorithms, finally helps to optimize the solution results without any experimentation on physical models or prototype. The flow visualization characteristic of the code inside the domain make it very power-full tool in the research field and other areas. There are some governing equations are associated with the flow field and it is typically or may not possible to apply directly those equations with many variables to model. CFD divide the flow domain into number of cells and solve the governing equations for the each cell by converting PDE's into algebraic form.

The accuracy and validity of the CFD depends upon the number of factors: quality of mesh, models or type of boundary conditions entered by the user, convergence criteria level and significant of the obtained results. As we know that the physical aspects of the flow field are based on three fundamental principles are:

Mass conservation equation

$$\frac{\partial \rho}{\partial t} + \nabla(\rho \vec{v}) = S_m \quad \text{... (3.1)}$$

For 2D axis symmetric the continuity equation

$$\frac{\partial \rho}{\partial t} + \frac{\partial}{\partial x}(\rho v_x) + \frac{\partial}{\partial r}(\rho v_r) + \frac{\partial \rho v_r}{r} = S_m \quad \text{... (3.2)}$$

Momentum conservation equation

$$\frac{\partial}{\partial t}(\rho \vec{v}) + \nabla.(\rho \vec{v}\, \vec{v}) = -\nabla \mathrm{p} + \rho \vec{g} + \vec{F} \quad \text{... (3.3)}$$

Energy equation

$$\frac{\partial}{\partial t}(\rho E) + \nabla.(\vec{v}\,(\rho E + p)) = -\nabla.\left(\sum_{\mathrm{j}} \mathrm{h_j J_J}\right) + S_h \quad \text{... (3.4)}$$

These fundamental principles are generally expressed in integral and partial derivative form in mathematics but CFD solve these fundamental equations by converting these into algebraic form and obtain the flow field solutions according to the desired conditions and input parameters. For the repetition or to change the CFD solution required a high-speed computer. The several CFD software packages are available such as Fluent, Comsol, CFX, CFDRC etc. for the simulation purposes.

3.1 DISCRETIZATION TECHNIQUES

In the discretization methods the governing equations are converted from partial differential and integral form to algebraic form. The various types of the dicretization methods are used in the CFD code.

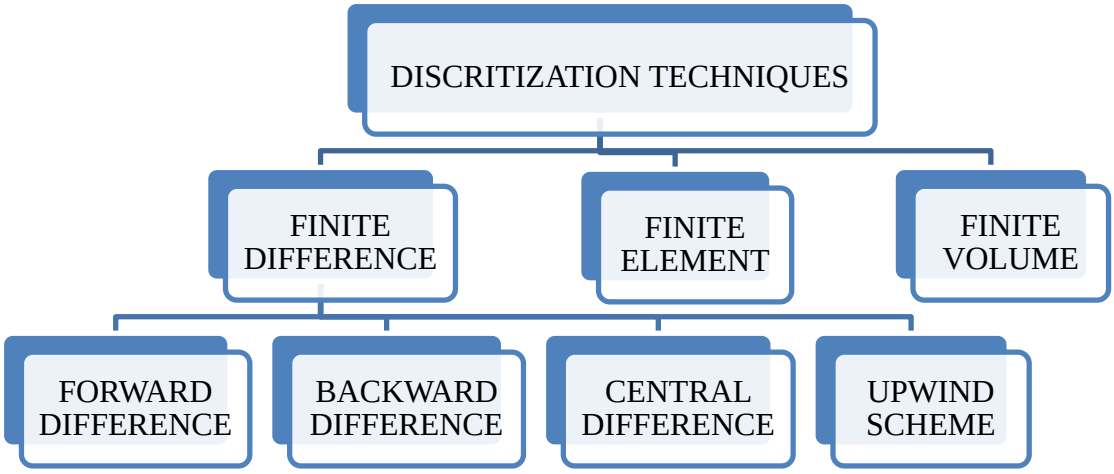

Figure 3.1: Discritization methods

a) Finite difference method

Finite difference method is one of the most common methods to obtain the numerical solution in CFD. At each node of the grid the fluid flow domain is defined and Taylor series is used for the expansion. In one dimensional flow problem simple differential equation gives smooth and analytical solution with boundary conditions.

b) Finite element method

The main feature of the FEM is that the simple piecewise polynomial functions used the elements to describe the variation of unknown flow variables. The associated error are measured by the weighted residuals concept and minimized later. The approximate solution is obtained from the non-linear equations. Any complex or any shaped geometry can be deal with this method.

c) Finite Volume Method

The conservation equations of integral form are discretized by finite-volume method in physical space. Finite volume method is concern with control volume not with grid intersections and type of grid is accommodated by itself. Generally an unstructured type grid is used instead of structured grid because it allows the option for defining the location and shape of the control volumes. But the boundaries of control volume are defined by the grid.

3.2 CFD SIMULATION PROCESS

CFD simulation is process to get the solution, information about the flow field inside, around and over any simple or complex geometry. So the few steps have been derived to complete the process. Those steps are given below.

a) Preprocessing

It is initial stage of the simulation in which modeling and meshing is done over the flow domain.

- **Modeling**

  In the modeling the flow domain or geometry is created in the various codes like GAMBIT, ANSYS, and COMSOL etc. as per the dimensions of the model. The modeling of the flow domain may be 2D and 3D depends upon the user.

- **Meshing**

  In the mesh generation, the flow domain is discretized into small number of elements. The size of the mesh is selected after the grid independence test. In this test grid size is varied until the constant or almost equal results does not obtained. Although with fine mesh more accurate solutions are obtained than course size mesh but long computing time and more power is consumed.

b) Solver

It is the secondary stage of the CFD analysis process in which the all the physical boundary conditions, flowing materials, flow parameters, convergence criteria etc. are assigned or set up to get the solution.

c) Post processing

It is final stage of the CFD-analysis process in which iterations are performed and after the completion of the iterations the results in the form of contour and vectors are plotted

3.3 ADVANTAGES AND DISADVANTAGES

a) Advantages

- Widely used in industrial application and research areas.
- Flexibility to change the simulation results without any physical change in the model.
- Approximate or close results can be observed without any experimentation on model.
- Reduction in the cost of physical models or prototype.

b) **Disadvantages**

- Numerical errors are during the solving the problem in computer.
- Actual physical initial and boundary condition are required to simulate the problem.
- Super computer or work station is required for the analysis of complex flow field.

3.4 APPLICATIONS

- Aerodynamics vehicles like aircrafts and missiles
- Heat transfer industrial purposes like boiler, heat exchanger
- Electronic appliances
- Hydrodynamics system
- Fluid flow fields like pipe, bends, pumps etc.
- Maine engineering
- Environmental engineering

- Sports
- Chemical engineering
- Automobile engineering
- Civil engineering

3.5 TURBULENCE MODELS

Turbulence is undesired vortices or unsteadiness in the flow regimes or flowing fluid due to change in the properties like momentum diffusion, variation in pressure and velocity with respect to space and time. The Reynolds number of the flow gives the complete information of inertia and viscous force associated with the flow field. Therefore some types of turbulence models are given below which are used in various applications.

a) Classification of turbulence models

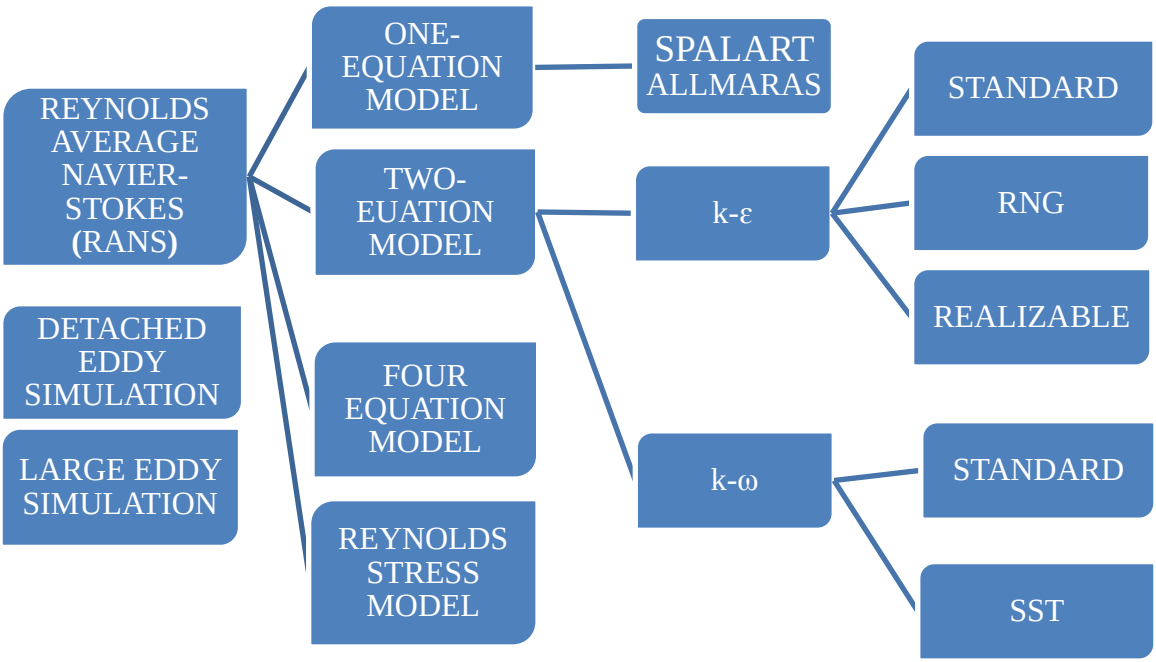

Figure 3.2: Turbulence models

b) Turbulence models and their usage

- Spalart Allmaras: generally used for 2-D problem with coarse mesh size.

- Standard k-ε: this model is mostly used where the pressure gradient is less and minor separation is occurred.
- Realizable k-ε: The model is suitable for the complex shear flow and also associated with transient or swirl flow.
- Standard k-ω: the turbulent model which is used for complex flow, wall boundary layer, low Reynolds number. Also may be where adverse pressure gradient and high separation is taking place.
- SST k-ω: Due to dependency on wall distance not suitable for shear flow type problems. Very similar to Standard k-ω model.
- RSM: Mostly used for 3-D and complex geometry and also suitable for streamline curvature type and strong rotating flow field.

3.6 MULTIPHASE FLOW REGIMES

Several types of flow exist in the nature but now days the technology is for multiphase flow or mixture of physical matters like gas, liquid, solid. The multiphase flow is encountered in wide range of the world. In multiphase flow study of the each is done to identify the interaction of physical matters with the flow and flow field within the flowing region. Types and application of multiphase flow regimes are given below:

a) Gas liquid flow or liquid-liquid flow

- The flow of gas or fluid bubbles in a continuous phase is known as bubbly flow like absorbers, aeration, air lift pumps, cavitation, evaporators, flotation and scrubbers.
- Flow of fluid droplets in the continuous phase called as droplet flow. Example absorbers, atomizers, combustors, cryogenic pumping, dryers, evaporators, gas cooling and scrubbers.
- Flow of large bubbles in the continuous phase is called as slug slow.
- Flow of immiscible fluids is known as stratified or free flow. Boling and condensation in nuclear reactors.

b) Gas - solid flow

- Particle- laden flow: the discrete solid particles flow in the continuous gas flow field. Cyclone separators, air classifier, dust collectors.
- Pneumatic transport depends upon the solid loading rate, Reynolds number and the properties of the solid particles. Mostly dune, slug and homogeneous type flow are found in practices applications. Transportation of cement and metal powders etc.

c) Liquid solid flow

- Slurry flow: the flow solid particles in the liquid. Generally the stokes number in the slurry flow is < 1and if the stokes number is >1 the characteristics of flow becomes fluidization.
- Hydro-transport: the densely distributed solid particles in the continuous flow. Example: mineral processing.
- Sedimentation: a tall column in which initially the solid particles are uniformly suspended/dispersed in the mixture. After interval of time the particles starts to settle down gradually and form sludge layer and at the top clear interface exists. A constant settling zone is formed near the centre.

d) Three phase flow: the combination of the all three phases i.e. solid, liquid, gas.

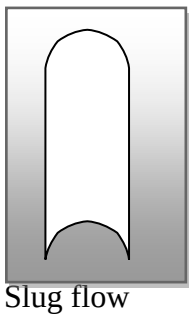

a) Slug flow

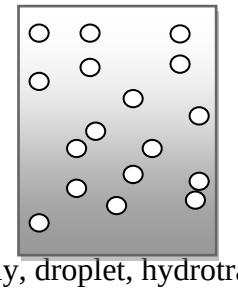

b) bubbly, droplet, hydrotransport or slurry flow

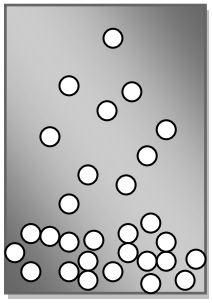

c) Sedimentation

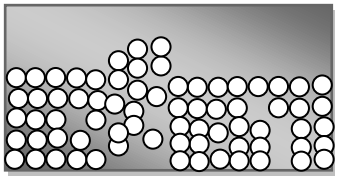

d) fluidized bed

Figure 3.3: Different types of flow regimes

3.7 MULTIPHASE MODELS APPROACHES

In the multiphase models there are three types of approaches are used to simulate the multiphase problem.

Euler –Euler approach: In this approach all the phase are treated as a continuum phase. The volume of the other phase is negligible and the introduced volume fractions are assumed to be functions of time and space and the sum of the fraction is equal to one. Conservation equations are solved for each phase in similar fashion and obtained set of equations. Three type of Euler- Euler multiphase models are:

3.7.1 Volume of fluid

The VOF solve the single set of momentum equations to model the two or more than two immiscible fluid and track the volume fraction of each phase in the flow region.

Application: stratified flow, free surface flows, filling, sloshing, large bubbles motion in the liquid, the motion of liquid after dam breakage.

3.7.2 Mixture model

This model is used for the multiphase or homogeneous flow by assuming the same velocity of the secondary phase. The model is imposed with suitable coupling between the phases and also used for non-Newtonian type of flow.

The mixture model can solve n number of phases by solving the continuity, momentum and energy equations for the each phase, volume fraction and other algebraic equations. The mixture model is extensively used for solid- liquid flow.

Application: cyclone separators, sedimentation, particle laden and bubbly flow when gas volume fraction is low.

3.7.3 Eulerian model

The model solves the set continuity and momentum equations for n number of phases. The model in which coupling is made due to pressure and inter-phase exchange. The solution is obtained separately for each phase. Firstly the continuum phase is treated and then for the solid or granular phase.

Applications: particles suspensions, risers, fluidized beds and bubble columns.

a) Volume fraction equation

The equation for the defining the volume fraction of the solid phase is given by:

$$V_q = \int a_q \, dV \qquad \ldots (3.5)$$

where

$$\sum_{q=1}^{2} a_q = 1 \qquad \ldots (3.6)$$

Where the effective density of phase q is

$$\tilde{\rho} = a_q \rho_q \qquad \ldots (3.7)$$

b) Continuity equation for the solid phase

$$\frac{d}{dt}(a_q \rho_q) + \nabla(a_q \rho_q v_q) = \sum_{p=1}^{n} (\dot{m}_{pq} - \dot{m}_{qp}) + S_q \qquad \ldots (3.8)$$

$\dot{m}_{pq}$ Characterizes the mass transfer from phase q to phase p

Source term S_q= 0 in equation 3.8.

c) Momentum equation for liquid phase

$$\frac{d}{dt}(a_l \rho_l \vec{v}_l) + \nabla(a_l \rho_l \vec{v}_l \vec{v}_l) = -a_l \nabla p + \nabla \bar{\bar{\tau}}_l + a_l \rho_l \vec{g} + K_{sl}(\vec{v}_s - \vec{v}_l) \qquad \ldots (3.9)$$

d) Momentum equation for solid phase

$$\left(\frac{d}{dt}(a_s \rho_s \vec{v}_s) + \nabla(a_s \rho_s \vec{v}_s \vec{v}_s)\right.$$
$$\left. = -a_s \nabla p - a_l \nabla p_s + \nabla \bar{\bar{\tau}}_s + a_s \rho_s \vec{g} + K_{sl}(\vec{v}_l - \vec{v}_s)\right) \qquad \ldots (3.10)$$

$$p_s = a_s \rho_s \theta_s + 2\rho_s (1 + e_{ss}) a_s^2 g_{o,ss} \theta_s \qquad \ldots (3.11)$$

Cofficient of restitution for the collision of particles taken as 0.9 and granular temmperature is proportion to the kinetic energy of fluctuating particles.the distribution function shows the transient condition at which the spacing betwwen the particles decreases continue to incompressible condition.the probability of the collision between the grains when solid particles becomes dense ang given by:

$$g_{o,ss} = \left[1 - \left(\frac{a_x}{a_{x,max}}\right)^{\frac{1}{3}}\right]^{-1} \quad \ldots (3.12)$$

Phase stress tensor for solid is given by

$$\bar{\bar{\tau}}_s = a_s\mu_s\left(\nabla\vec{\vartheta}_s + \nabla\vec{\vartheta}_s^{tr}\right) + a_s\left(\lambda_s - \frac{2}{3}\,\mu_q\right)\nabla\vec{\vartheta}_s \quad \ldots (3.13)$$

Phase stress tensor for liquid is given by

$$\bar{\bar{\tau}}_l = a_l\mu_l\left(\nabla\vec{\vartheta}_l + \nabla\vec{\vartheta}_s^{tr}\right) \quad \ldots (3.14)$$

Bulk viscosity of solid is

$$\lambda_s = \frac{4}{3}\,a_s\rho_s\,d_s g_{o.ss}(1 + e_{ss})\left(\frac{\theta_s}{\pi}\right)^{\frac{1}{2}} \quad \ldots (3.15)$$

Shear viscosity of solid

$$\mu_s = \mu_{s,col} + \mu_{s,skin} + \mu_{s,fr} \quad \ldots (3.16)$$

Collisional viscosity

$$\mu_{s,col} = \frac{4}{5}\,a_s\rho_s\,d_s g_{o,ss}(1 + e_{ss})\left(\frac{\emptyset_s}{\pi}\right)^{\frac{1}{2}} \quad \ldots (3.17)$$

kinetic viscosity

$$\mu_{s,kin} = \frac{10\rho_s\,d_s\sqrt{\theta_s\pi}}{96a_s\,(1 + e_{ss})g_{o,ss}} + \left[1 + \frac{4}{5}\,a_s\rho_s\,d_s g_{o,ss}(1 + e_{ss})\right]^2 a_s \quad \ldots (3.18)$$

Frictional viscosity

$$\mu_{s,fr} = \frac{P_s\sin\varphi}{2\sqrt{I_{2D}}} \quad \ldots (3.19)$$

Liquid solid exchange coeeficient, $K_{sl} = K_{ls}$

$$K_{ls} = 150\,\frac{a_s(1+a_l)\mu_l}{a_l d_s^2} + 1.75\,\frac{\rho_l\,a_s|\vec{v_s} - \vec{v_l}|}{d_s} \quad \ldots (3.20)$$

3.8 DISCRETE PHASE MODEL

Advanced Computational fluid dynamics provides the solution for multiphase flow with two different approaches: Euler-Euler and Euler-Lagrange.

3.8.1 Euler-Lagrange

In this approach the carrying fluid is behaved as a continuum phase by solving the Navier-Stokes equations, dispersed or discrete phase is solved by tracking the large numbers of particles, droplets and bubbles in the calculated flow field. The discrete phase can exchange the mass, momentum and energy with the carrying fluid.

When the particle-particle interaction is neglected and very low volume fraction of dispersed phase in the flow field although high mass loading ($m_{particle} \geq m_{fluid}$) is acceptable, the approach is considered simpler one. Hence the particle or droplet is tracked individually at specified time of interval after calculation of the fluid flow. This approach is applicable for simulation of coal, spray dryers and particle flow, but not applicable where volume fraction is not neglected.

3.9 EQUATION OF MOTION OF PARTICLE

a) Partial force balance

Fluent predicts the trajectory of particle of discrete phase by integrating the force balance equation (Lagrangian frame) on the particle. The force balance equation can be written as

$$\frac{du_p}{dt} = F_D(v_f - v_p) + \frac{g(\rho_p - \rho_f)}{\rho_p} + F \quad \ldots (3.21)$$

Where, F is the force per unit particle mass, $F_D(v_f - v_p)$ is drag force per unit particle mass and

$$F_D = \frac{18\mu_f}{\rho_p d_p^2}\frac{C_D Re}{24} \quad \ldots (3.22)$$

$$Re \equiv \frac{\rho_f d_p |v_p - v_f|}{\mu_f} \quad \ldots (3.23)$$

b) Turbulent dispersion of particles

Due to the turbulence in the fluid the dispersion of the particles can be predicted with stochastic rebound model or particle cloud model. The effect of turbulent velocity fluctuations on the particle trajectory is incorporated by stochastic or random walk model.

Where, the particles cloud about the mean trajectory is evaluated by the particle cloud tracking model.

c) Stochastic Tracking

In the turbulent flow, the particle trajectories are predicted by the mean fluid phase velocity, v_f given in the equation of trajectory

$v_f = \overline{v_f} +$

$v_f^{'}$ ... (3.24)

In this equation, the value of fluctuating velocity of the gas flow can be incorporated to evaluate the dispersion of the particle due to the turbulence effect. In fluent the turbulent dispersion on the particle is evaluated by integrating the trajectory equation for the each particle by using the fluctuating velocity $\overline{v_f} + v_f^{'}$ while integrating.

3.10 PARTICLE EROSION MODEL

Particle erosion and accretion can be predicted at boundaries wall. The erosion rate is given by:

$$R_{erosion} = \frac{\sum_{p=1}^{N_{particles}} m_p C(d_p) f(\alpha) {v_q}^{b(v_p)}}{A_{face}} \quad \text{... (3.25)}$$

Default values of constants are: $C = 1.8 * 10^{-9}$, $b = 0$, and $f = 1$.

Limitations of discrete phase model

- **Limitation of particles volume fraction**

  In this the particles volume fraction is generally upto10-12% and mass flow of particles may be more than 10-12% or may be equal to mass flow for continuum flow.

  The interaction between particle-particle is neglected in case of gas flow.

- **Limitation on modeling continuous suspensions of particles**

  This approach is applicable when the particles are injected separately from the appropriate entrance into the continuous phase and exit is well defined for the particles.

  It cannot be applicable for mixture (solid-liquid) or suspension of the solid particles into continuous phase.

3.11 TRANSPORTATION OF SLURRY

Transportation of slurry is a phenomenon in which solid-liquid mixture pumped by slurry pump, is transfer to particular site through pipe-line system. The selection of pump depends upon the pressure discharge and abrasivity. The most common and cheapest type of slurry pump is Centrifugal Slurry Pump. Example: Ash-water slurry, coal-oil slurry at thermal power plants.

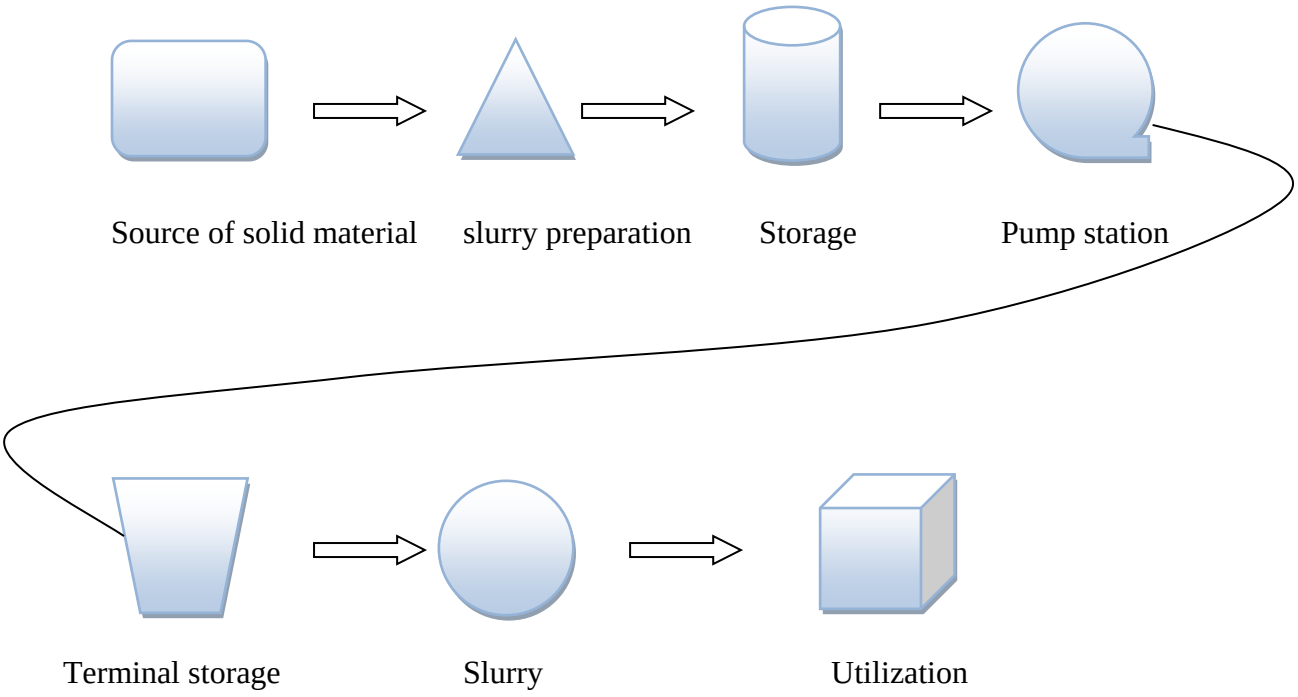

Figure 3.4: Transportation of Slurry

The solids may be transported by two mechanism by hydraulic and by pneumatic transportation system. In the hydraulic system the slurry (mixture of solid liquid) is transported through the pipe line in the various industries and power plants whereas in pneumatic system the solids particulates are transported with the help of carrier fluid

compressed air. A flow diagram is shown for a thermal power plant in which the material is flow from the source of solid to utilization place.

During the transportation of the solid particulates through the pipe line erosion of the pipe-line system exist due to the high velocity and impacts of solid particulates of the wall of pipe line. Hence to evaluate the intensity of the erosion with the bottom ash slurry, a numerical investigation has been made using the multiphase model Discrete phase which helps to evaluate the erosion rate in the flow field by tracking the solid particulates flowing through the system.

CHAPTER 4 SOLID LIQUID EROSION WEAR USING CFD

In the present work, CFD multiphase euler-lagrange model is used to identify the erosion rate and to analyze the effects of velocity, particles size, and solid concentration for the erosion wear in pipe-bend. The erosion wear takes place generally in power plants due to transportation of slurry (water-bottom ash) through pipe-line system due to high velocity and impacts of solid particulates over the wall of the flow domain.

4.1MODELING AND MESHING

a) Modeling of 90^o horizontal pipe bend

A 90^o horizontal pipe-bend of 100 mm diameter is modeled in the CFD code GAMBIT-2.3.16**.** The total length of the pipe is selected enough for fully developed flow. The detail and specification of the geometry is described in Table 4.1. Where D is the diameter of pipe-bend, r is the radius of the curvature, the bend measured from the centre line as shown in figure 4.1 and r/D is the ratio of the radius of the curvature to the diameter of the pipe.

b) Meshing of the flow domain

To evaluate the physical value and behaviour of flow at each section of the domain or flow field meshing is imposed on the domain. While meshing the fluid field is discritized into small number of elements. The meshing is categorized by shaped of the elements like hexahedral, tetrahedron, triangular elements etc.

In this work hexahedral-cooper type meshing is used to discritize the domain into small number of cell as shown in Figure 4.3 (a) and (b). Three different sizes of mesh are used for the grid independence test.

Table 4.1: Detail and Specification of the flowing domain

Geometry: Pipe-Bend			
Diameter, D (mm)	**r/D ratio**	**Total length, L (m)**	**Density (kg/m^3)**
100	1.5	1.5	7850 (Mild Steel)

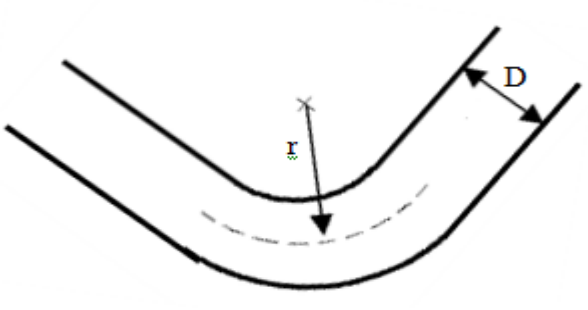

Figure 4.1: Schematic diagram of horizontal pipe-bend

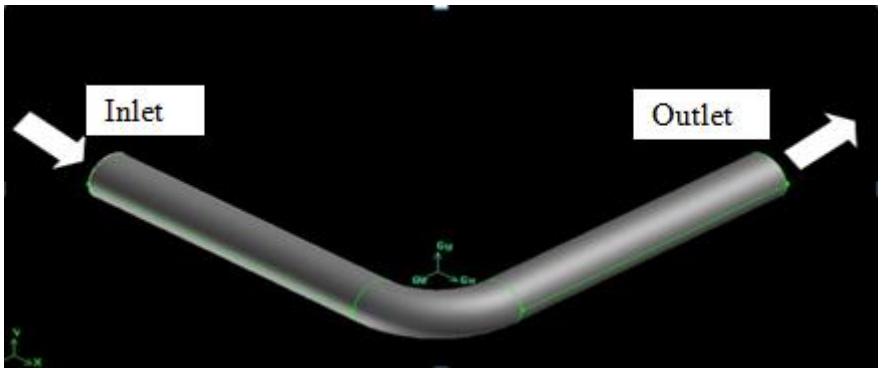

Figure 4.2: 90^0 horizontal pipe-bend

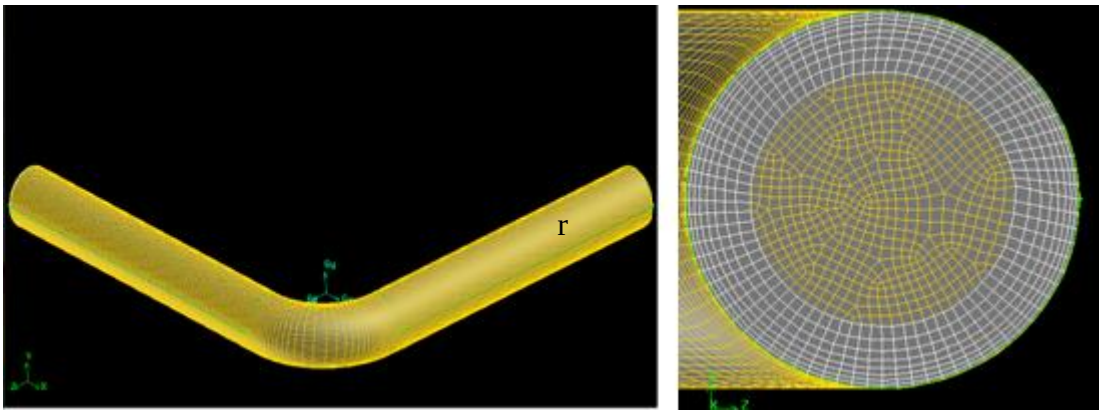

Figure 4.3: (a) Meshing on pipe-bend (b) Cross-section of pipe bend with mesh.

4.2 MATERIALS PROPERTIES

- **Properties**

The properties of the continuum media (water) and dispersed phase (bottom ash) are given the Table 4.2. The input parameters and conditions used in FLUENT for simulation the problem are described in the Table 4.4.

Table 4.2: Properties of liquid and solid phase

Liquid: Water		
Density (Kg/m^3)	**Viscosity (pa-s)**	
1000	0.001003	
Solid phase: Bottom ash **kumar et al. (2014)**		
Density (Kg/m^3)	**Particle size (µm)**	**Shape**
2220	162	Spherical/uniform

- **Grid independence test**

Grid independence is a technique which is used to select the optimized mesh size for the simulation process. The elements size is varied from coarser to finer with the same input parameters till the close or approximate same results do not observed. After selecting the mesh size the simulation process is carried out according to physical conditions and constraints.

Table 4.3: Grid independence

Mesh size (mm)	**Number of elements**	**Variation in erosion rate (kg/m^2-s)**
5	246810	Yes
4	433755	Yes
3	855000	No

4.3 BOUNDARY CONDITIONS AND INPUT PARAMETERS

The physical boundary conditions are imposed over the surfaces of flow field or domain for the simulation in fluent code. The type of the conditions are depends upon the flow field. Three boundary conditions which have been used are given in Table 4.4.

Table 4.4: Input models, parameters and boundary conditions for simulation

Type	Description	Input
Model	Turbulent model	• Standard k-ε • Standard wall function type.
	Discrete phase model	• Interaction with continuous phase • Maximum tracking in step • Physical model: erosion
Injection	Surface: inlet	• Velocity • Particle diameter • Solid mass flow rate • Stochastic model
Materials	Properties	• Flowing fluid • Solid domain • Solid phase
Operating conditions	Gravitational acceleration	• -9.81 in vertical downward
Boundary condition	Inlet	• Velocity inlet
	Outlet	• Pressure outflow
	Wall	• No-slip • DPM: Reflect type-Coefficient of restitutions for: Normal and tangential • Erosion model angle function: piece wise linear • Diameter function: constant • Velocity exponent function: constant

Solution controls	Discretization	• Pressure : standard • Momentum: first order upwind • Turbulence kinetic energy: first order upwind • Turbulence dissipation rate: first order upwind

Simulation of the solid-liquid phase is carried out to predict the erosion rate and to evaluate the effect velocity, solid concentration and particle size using the discrete phase model. Model which solve the erosion model equation and track the solid particulates in the fluid flow. Water is used as a carrier fluid and bottom ash particulates as a dispersed phase. Also to evaluate the effects of the velocity, solid concentration and particle size are varied from ranges 0.5 to 2.5m/s, 2.5% to 10% and 162 & 300μm respectively.

4.4 CFD SIMULATION AND VALIDATION

Erosion wear is material removal phenomenon due to impingement of solid particles over the surface which entrained through the carrier fluid like water. In thermal power plants bottom ash is transported in the slurry (ash-water) form with in the pipe line system which concerned with erosion wear. Various parameters are responsible for the erosion rate like impact angle, velocity, solid concentration, particle size etc. have been evaluated numerically using the erosion model in Computational fluid dynamics.

At low flow velocity the of the mixture in the flow field the solid particles starts to settle down in the flow field due to low inertia, low drag and gravitational force on the particles. Where the erosion wear in the flow field takes place **Bozzini et al. (2003)** as shown in Figure 4.4 (b). As the flow velocity is increased, the particles starts to strike at the outer wall of the pipe bend due to inertia and centrifugal force. Hence erosion magnitude and location shifts toward the outer wall along the pipe bend curve. At the same time the transverse motion of the particles the bend curvature and outlet where particles strikes over the wall lead to maximum erosion as shown in Figure 4.9.

High erosion rate is observed at the bend section than straight pipe due to variation velocity and impact angle of the particles **Wood et al. (2003)**. Along the bend curve angle is varying from the 0-90^{o}. The erosion wear is due to cutting action up-to impact angle 20-30^{o} and after that deformation action takes place leads to high erosion rate.

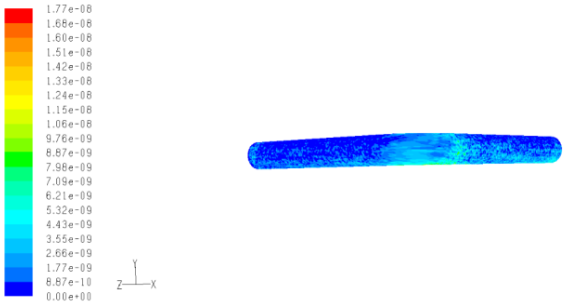

Figure 4.4.(a): Predicted erosion rate and magnitude

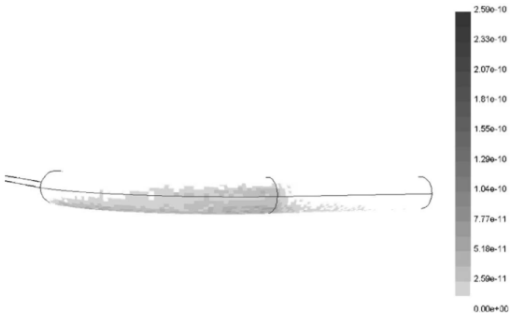

Figure 4.4.(b): Bozzini et al. (2003)

4.5 RESULTS AND DISCUSSION

4.5.1 Effect of impact velocity

The effect of velocity for the erosion wear of pipe-bend is analyzed at four different velocities 0.5 m/s, 1 m/s, 1.5 m/s 2 m/s and 5 m/s and represented in the graphical as well as pictorial form. The erosion rate is increases with increasing the velocity and also depends upon the intensity of increased velocity by assuming the constant others parameters like impact angle, solid concentration, target material, particle size etc.

It is observed that the erosion rate is gradually increases approximately from 2% to 20 % with increasing velocity of flowing mixture from 0.5 to 2m/s. Whereas steep erosion rate is observed means; by increasing very small velocity from 2 to 2.5 m/s erosion rate increases rapidly up-to 63% (approximate) than the other velocities for small particles while 52% (approximate) for coarser particles at all concentrations.

4.5.2 Effect of solid concentration

To evaluation of the effect of solid concentration in the erosion wear four different solid concentrations by weight are used viz. 2.5%, 5%, 7.5% and 10% in the present work. The total solid mass rate is used to examine the erosion rate at all the velocities and two particles size.

It is observed that very small or negligible effect of the solid concentration for the small and coarse particles size. Figures 4.7- 4.8 show almost same erosion rate at all flow rate and concentration for both the particles size. The erosion rate may also be different at other conditions with this particles size. But many authors and researchers have also found negligible and similar effect of particles size.

4.5.3 Effect of particles size

The study the effect of particles size in the erosion wear two particles size are considered i.e. 162μm & 300μm. At different velocity and solid concentration the numerical simulation is performed with these two sizes of particles.

The results shows that the particle size does not affect the erosion wear significantly for these two sizes of particles. The energy carried by the solid particle is increases with velocity at low concentration and leads to erosion. On the other hand number of particles decrease with increasing the particle diameter cause of erosion.

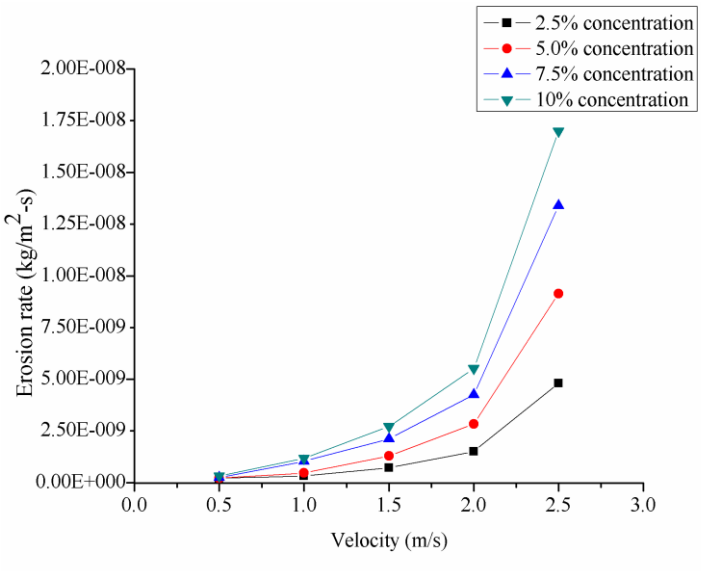

Figure 4.5: Erosion rate at different velocity and concentrations with 162μm particles

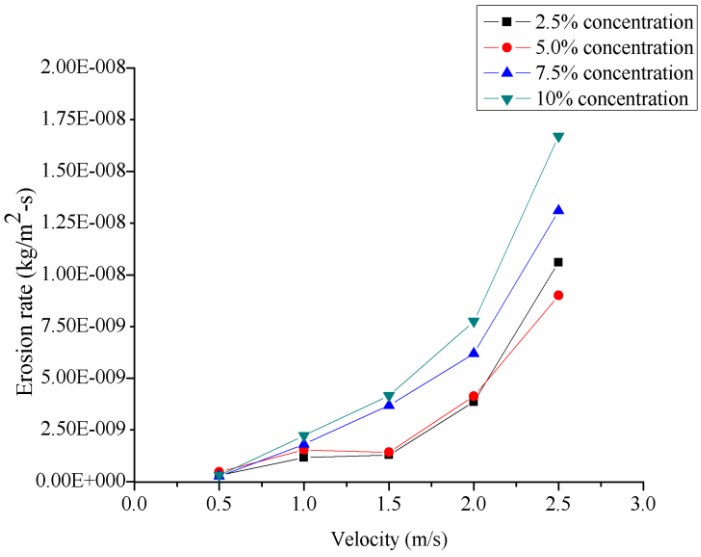

Figure 4.6: Erosion rate at different velocity and concentrations with 300μm particles

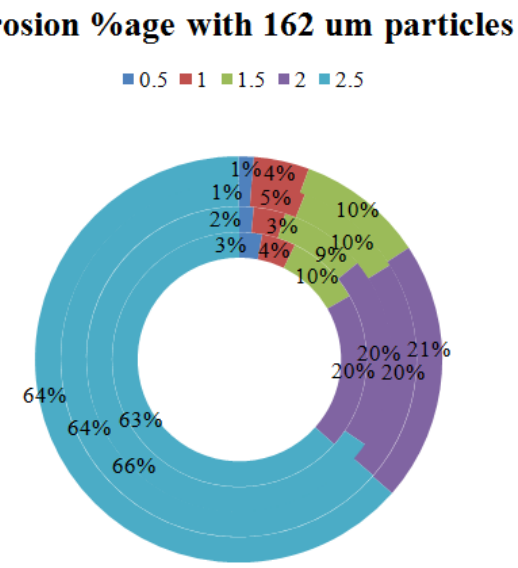

Figure 4.7: Erosion rate in percentage at different velocities (in angular direction) and concentrations (radially outward) with 162μm particles

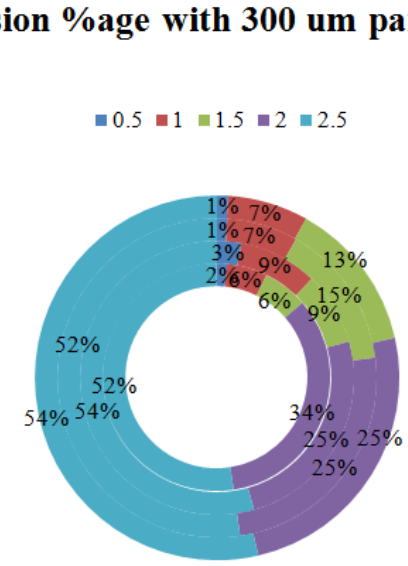

Figure 4.8: Erosion rate in percentage at different velocity (in angular direction) and concentrations (radially outward) with 300μm particles.

4.6 DISTRIBUTIONS

The distribution is the way to represent the fluid flow behaviour inside, around and at various sections of the flow field along with the intensity in the form of image. For example contours and vectors of pressure, velocity, turbulence, and erosion rate etc

a) Erosion rate distribution at pipe-bend wall

The contours for the erosion are plotted at the pipe bend wall at different velocities, solid concentrations and two particles sizes. The erosion magnitude is predicted for

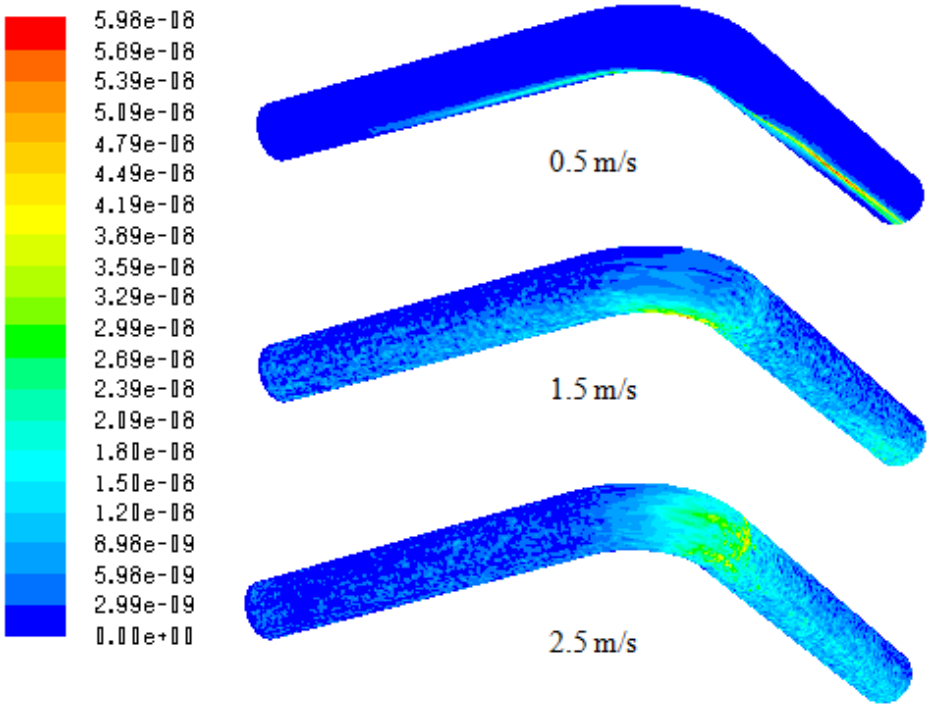

Figure 4.9: Erosion distributions at different velocities with 162μm particles size at 2.5% solid concentration

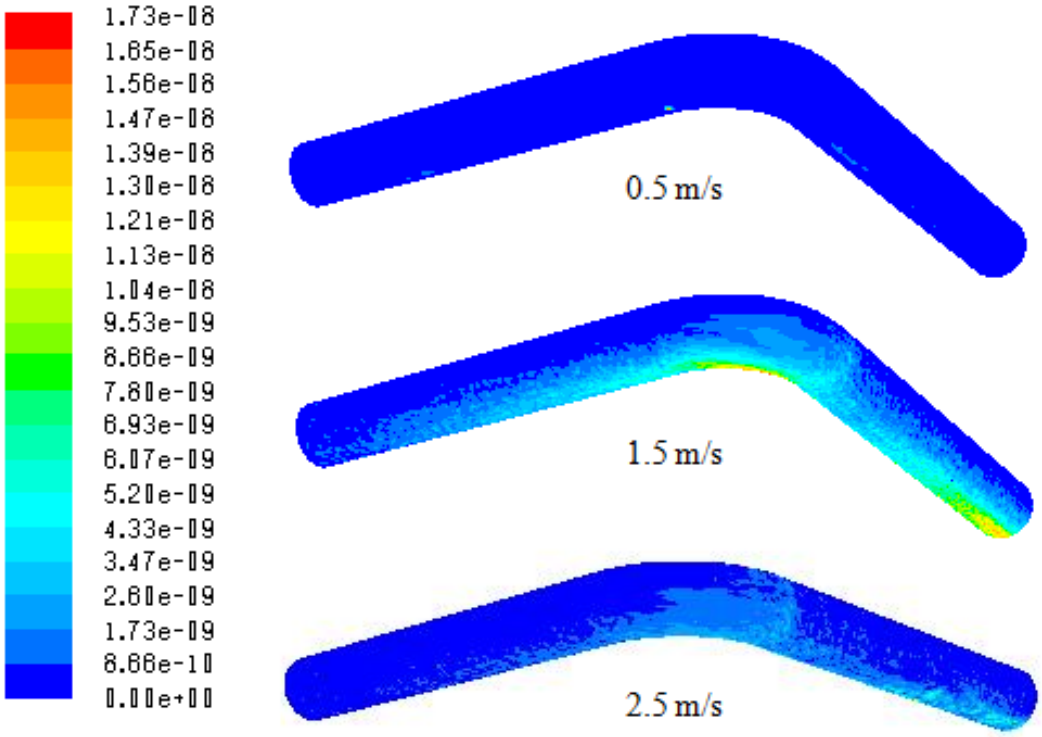

Figure 4.10: Erosion distributions at different velocities with 300μm particles size at 2.5% solid concentration

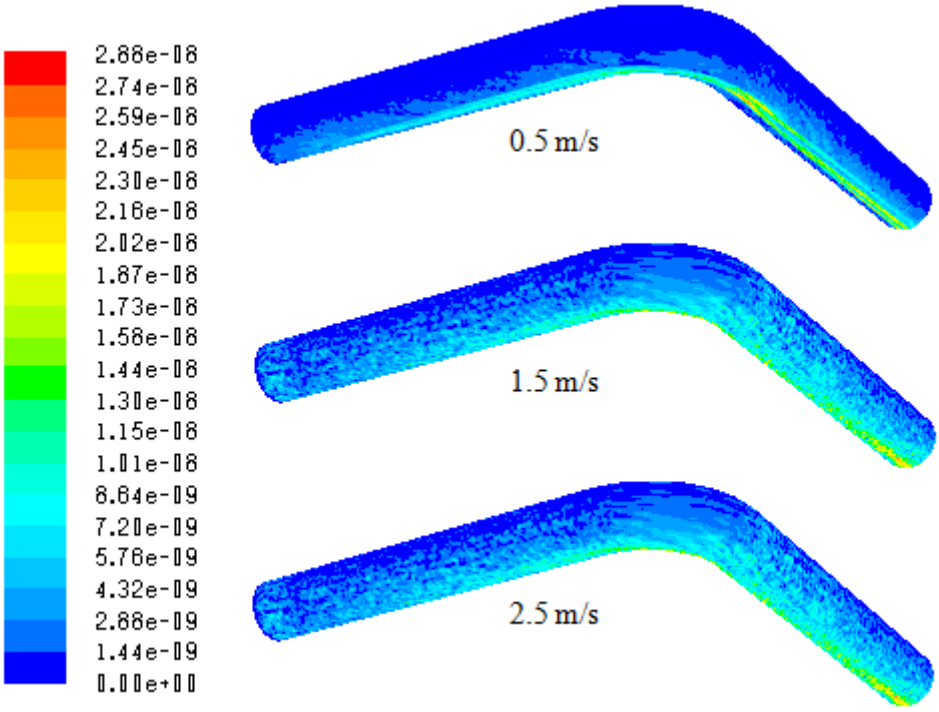

Figure 4.11: Erosion distributions at different velocities with 162μm particles size at 10% solid concentration

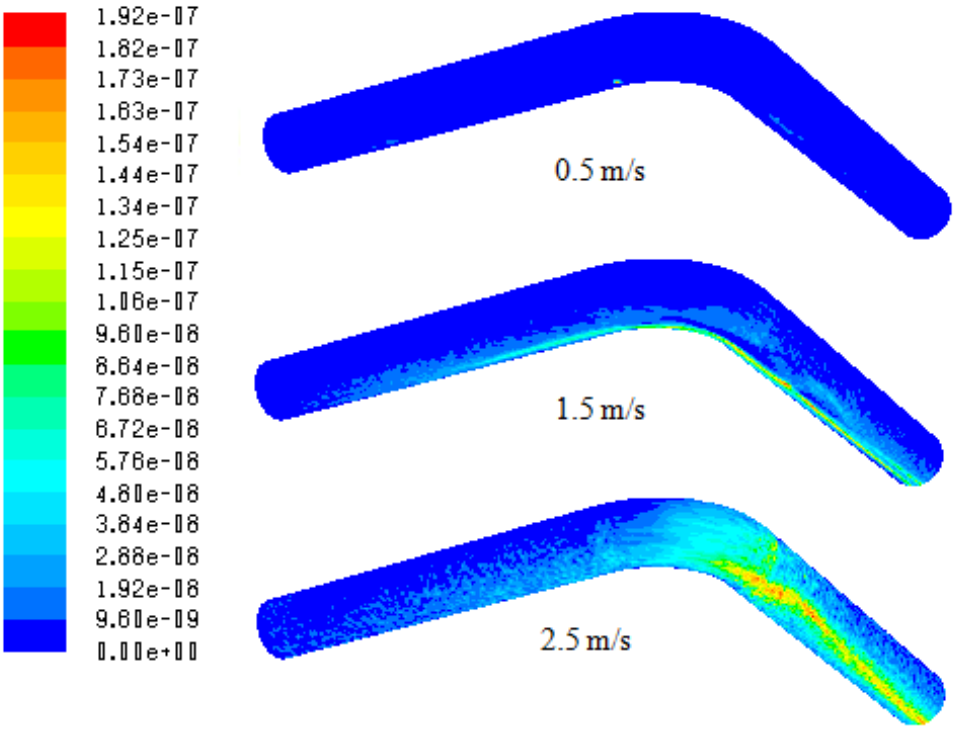

Figure 4.12: Erosion distributions at different velocities with 300μm particles size at 10% solid concentration

b) Velocity distributions

It is observed from the results that velocity at outlet of the bend section changes in transverse direction from inner wall to outer wall. Transverse recirculation of the flow takes place due to the centrifugal effect along the curvature of the bend. Due to this effect solid particles strikes at outer wall of the bend and lead to erosion at the impingement section as shown in Figure4. The recirculation in transverse plan is mainly depends upon the intensity of the velocity of the flowing mixture in the pipe-bend. Means low velocity low recirculation and high velocity means high recirculation takes place.

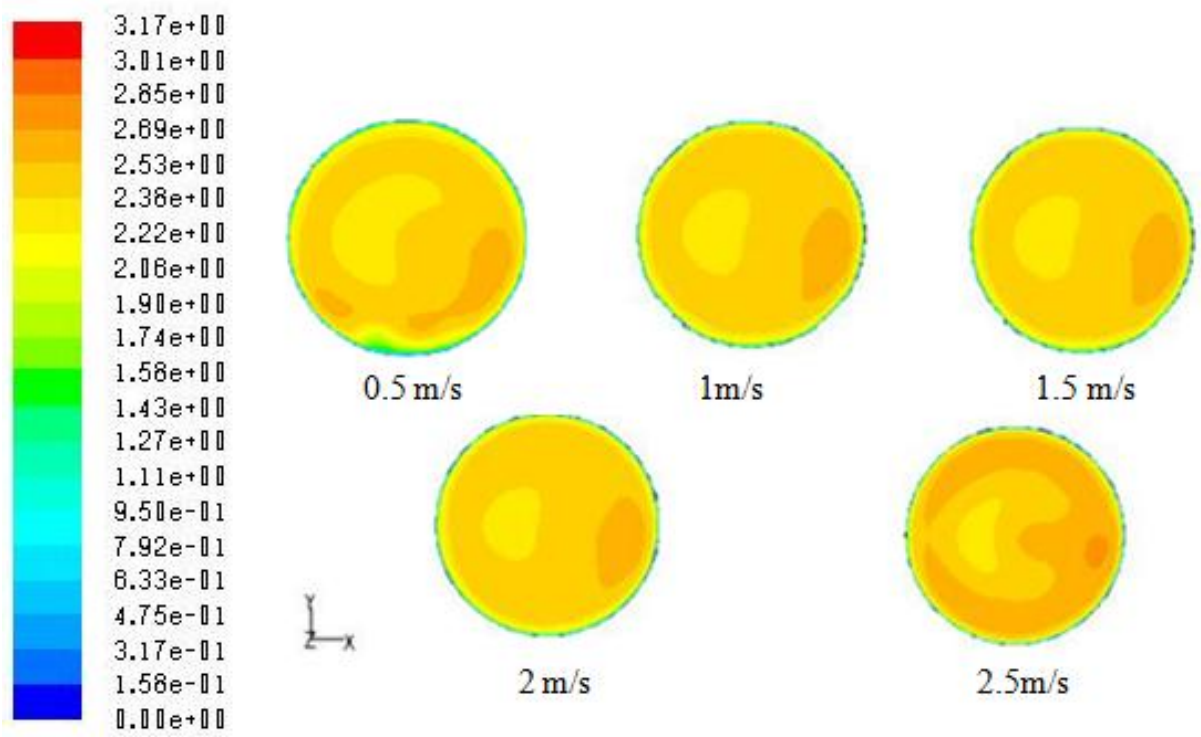

Figure 4.13: Velocity distributions at bend outlet with 162μm particles size at 10% solid concentration

c) Turbulence intensity at outer plane of bend

The turbulence intensity of the flowing fluid and solid depend upon the velocity. High turbulence intensity is occurred near the intrados of the bend. While low turbulence intensity near the extrados of the bend is observed. The f**igure** shows the turbulence intensity for the two sizes of particles. For the small particles turbulence is high at the center of the pipe-bend whereas high intensity is observed near the wall for the larger particles due to high weight of the particulates of solid at lower and high velocity. Almost same turbulence intensity for both the sizes of particles at velocity 1.5m/s

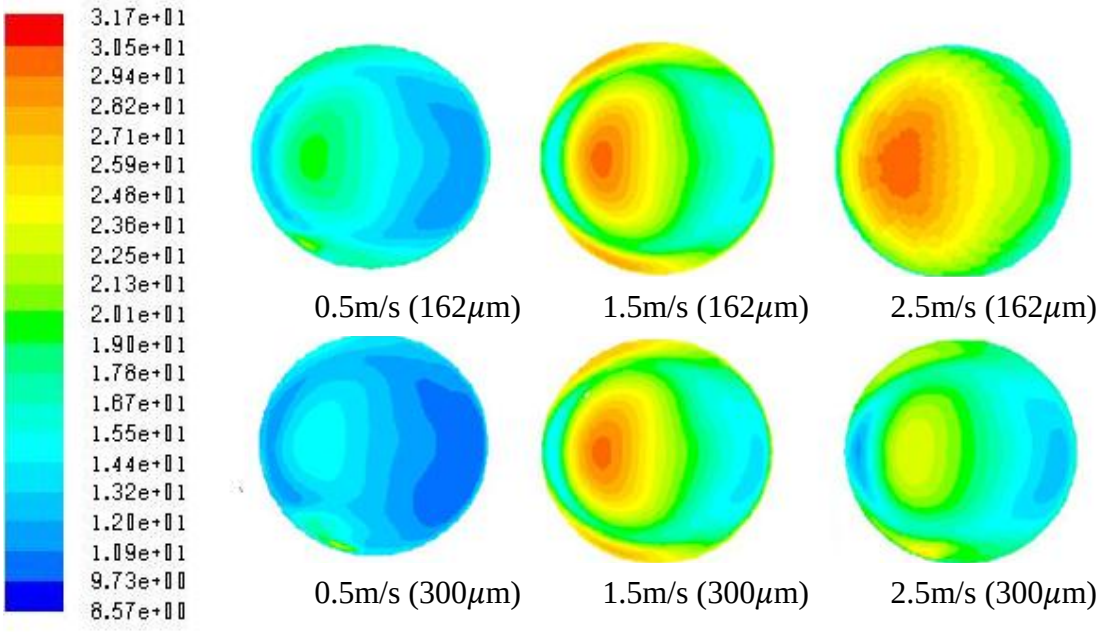

Figure 4.14: Turbulence intensity at outer plane of bend at different velocity and different particles size.

d) Velocity profiles at outer plane of bend

The distribution of the different velocities at outer plan of bend has been shown in Figures 4.15 – 4.19 for the velocity 0.5m/s to 2.5m/s. The velocity profile shows at good results at the particular velocity of the liquid and dispersed phase. The magnitude and intensity is varying from zero to maximum value.

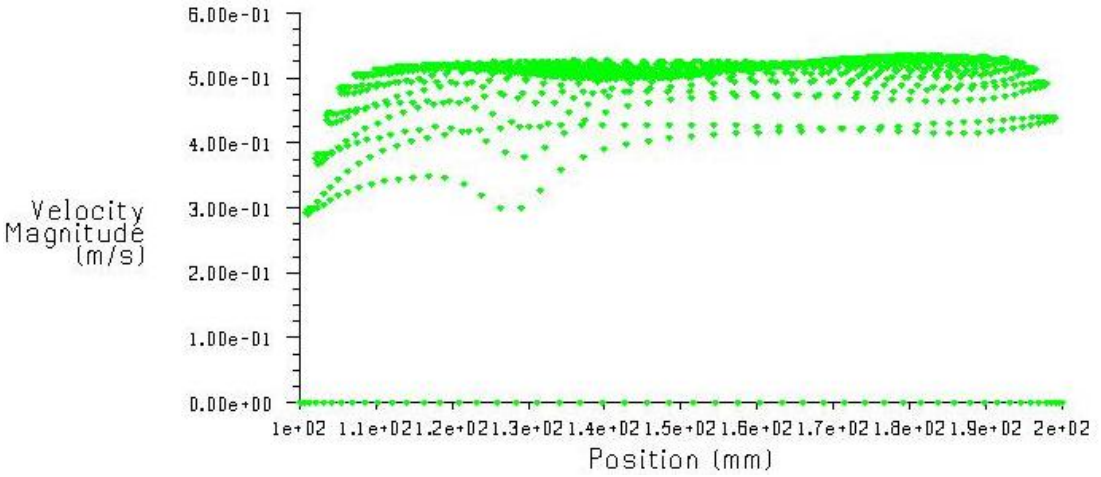

Figure 4.15: Velocity profile at bend outlet at velocity 0.5 m/s**.**

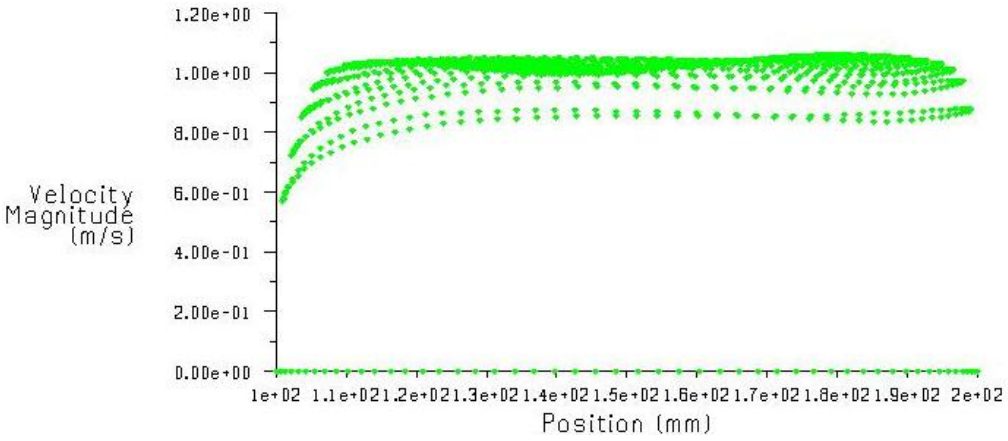

Figure 4.16: Velocity profile at bend outlet at velocity 1 m/s.

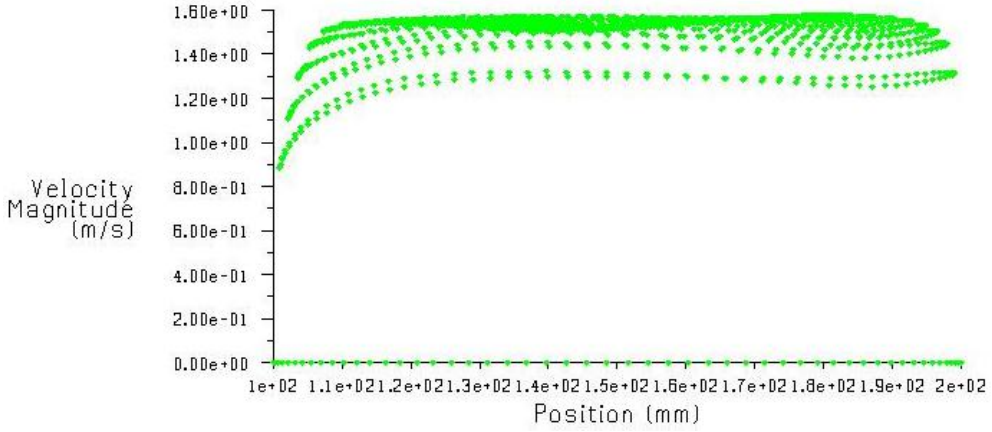

Figure 4.17: Velocity profile at bend outlet at velocity 1.5 m/s.

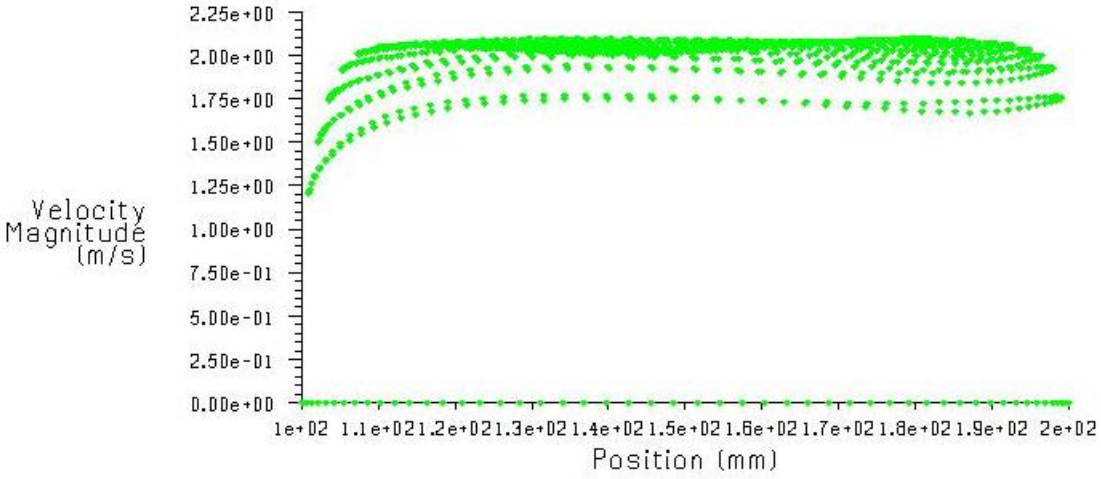

Figure 4.18: Velocity profile at bend outlet at velocity 2 m/s.

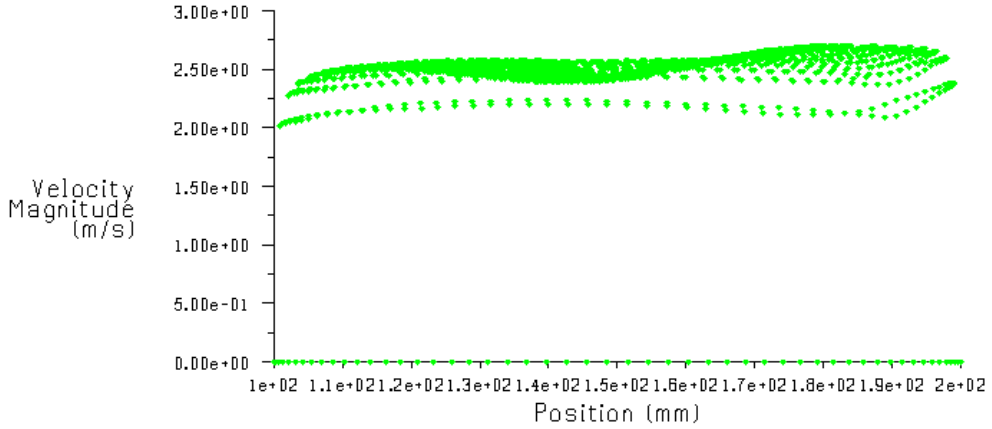

Figure 4.19: Velocity profile at bend outlet at velocity 2 m/s.

e) Magnitude and location of erosion at bend- wall and outer plane of bend.

The magnitude and the location of the erosion rate is plotted at the bend wall (green color) and outer plan (red color) of the bend. It is observed that at low velocity the maximum magnitude (9.24E-09) kg/m^2-s is at the bottom and (2.19E-09) kg/m^2-s at outer plan of the bend. Also the erosion rate is increasing with increasing the velocity as well shifting to new position at the pipe-bend wall. At velocity 1.5 m/s the erosion rate if observed near the extrados of the bend the maximum value 9.90 kg/m^2-s is found and at outer plane (5.98E-09) kg/m^2-s is observed. whereas at velocity 2.5m/s

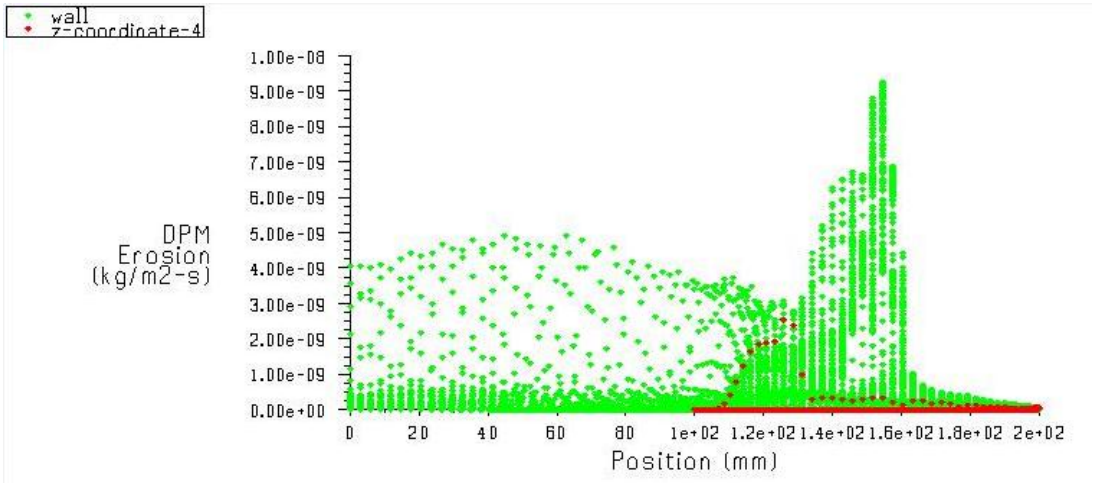

Figure 4.20: Magnitude and location of erosion at bend wall and outlet at velocity 0.5 m/s, concentration 2.5% and particle size 162 μm.

the erosion magnitude is found at the center of the extrados wall of the bend whose value is 4.81E-08 kg/m^2-s and 5.98E-08 kg/m^2-s at outer plane is found for the 162μm and 2.5% concentration. Similarly the magnitude and location is plotted for the larger particles and higher concentration.

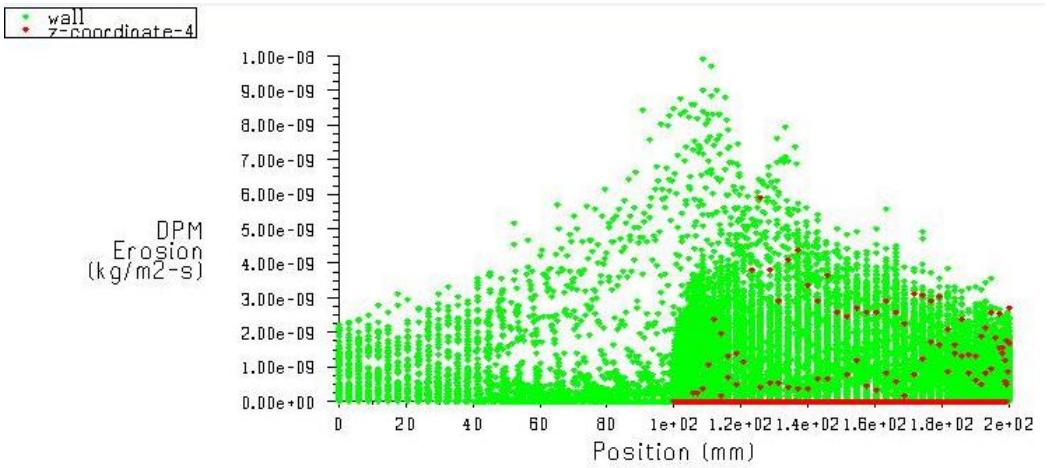

Figure 4.21: Magnitude and location of erosion at bend wall and outlet at velocity 1.5 m/s, concentration 2.5% and particle size 162 μm.

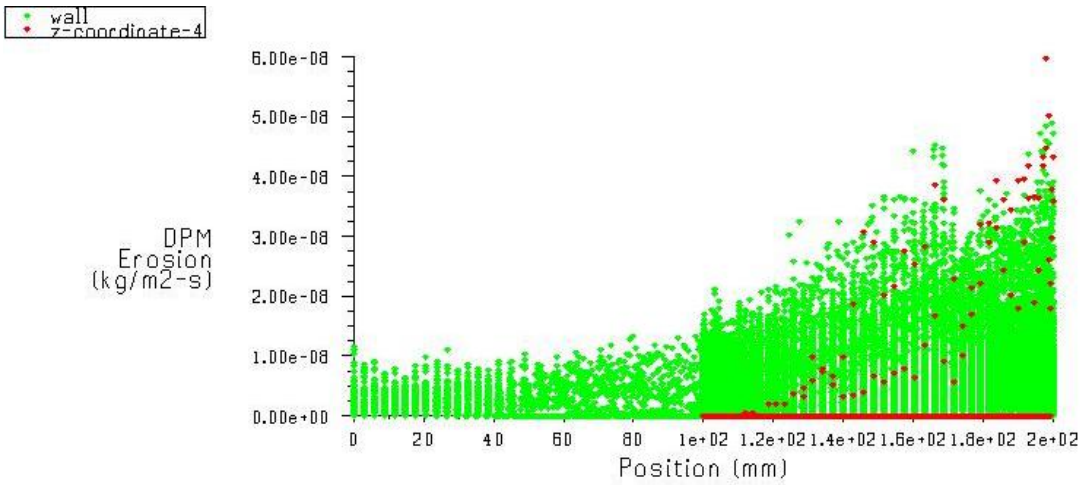

Figure 4.22: Magnitude and location of erosion at bend wall and outlet at velocity 2.5 m/s, concentration 2.5% and particle size 162 μm.

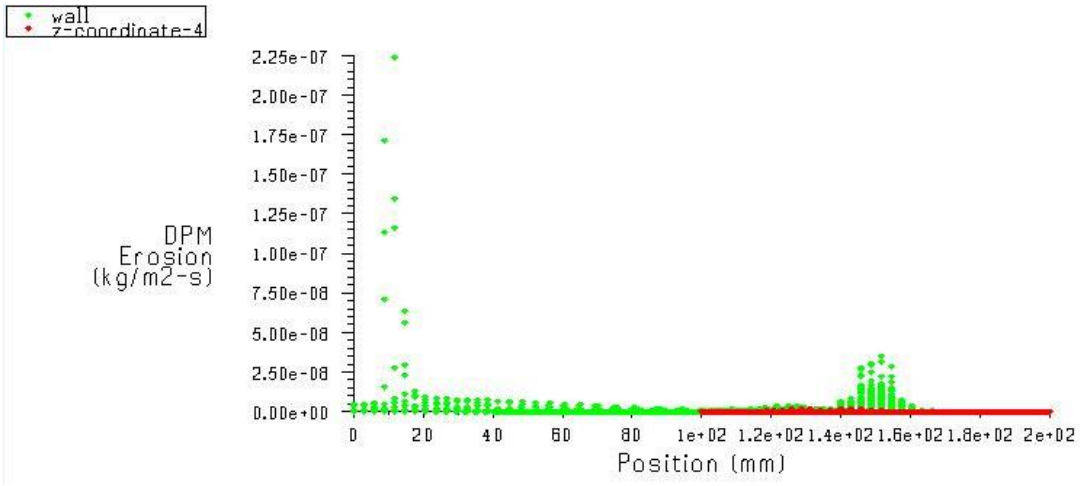

Figure 4.23: Magnitude and location of erosion at bend wall and outlet at velocity 0.5 m/s, concentration 2.5% and particle size 300 μm.

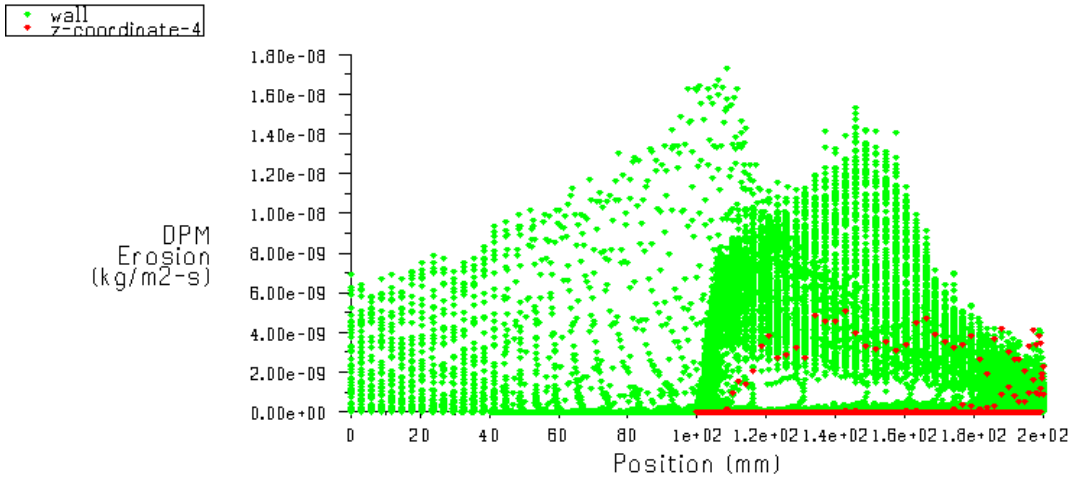

Figure 4.24: Magnitude and location of erosion at bend wall and outlet at velocity 1.5 m/s, concentration 2.5% and particle size 300 μm.

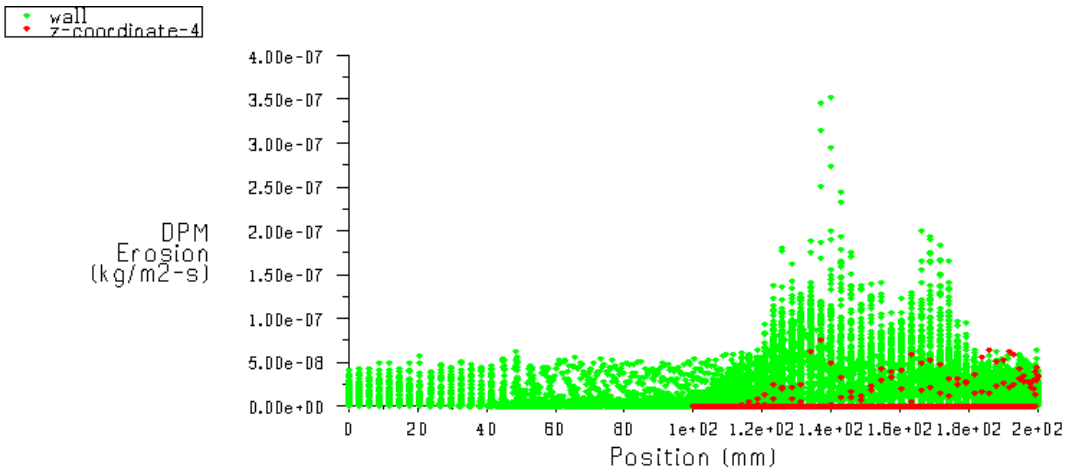

Figure 4.25: Magnitude and location of erosion at bend wall and outlet at velocity 2.5 m/s, concentration 2.5% and particle size 300 μm.

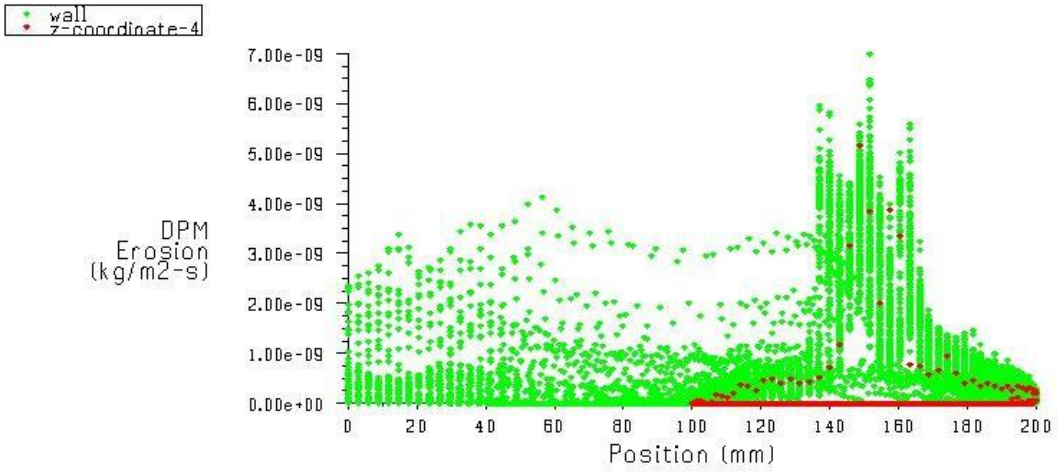

Figure 4.26: Magnitude and location of erosion at bend wall and outlet at velocity 0.5 m/s, concentration 10% and particle size 162 μm.

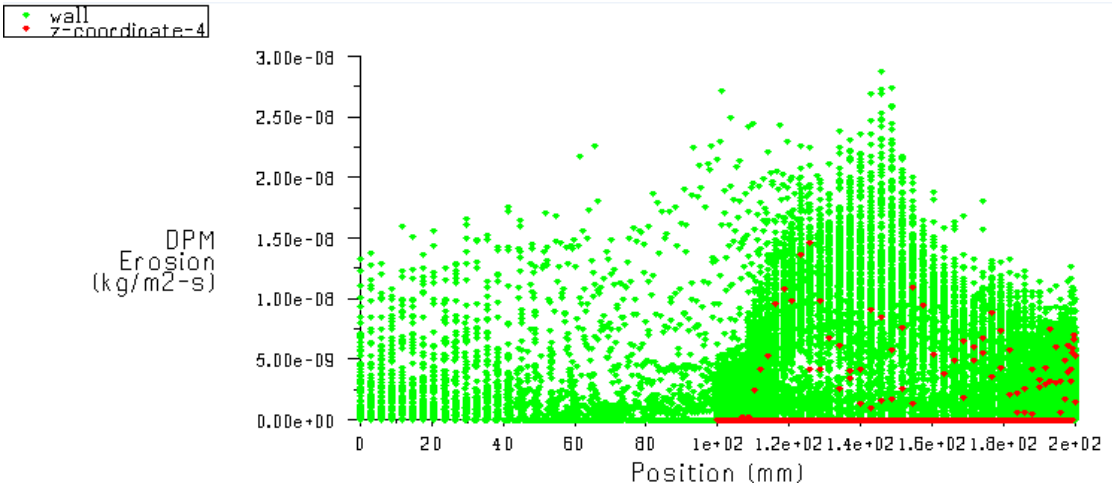

Figure 4.27: Magnitude and location of erosion at bend wall and outlet at velocity 1.5 m/s, concentration 10% and particle size 162 μm.

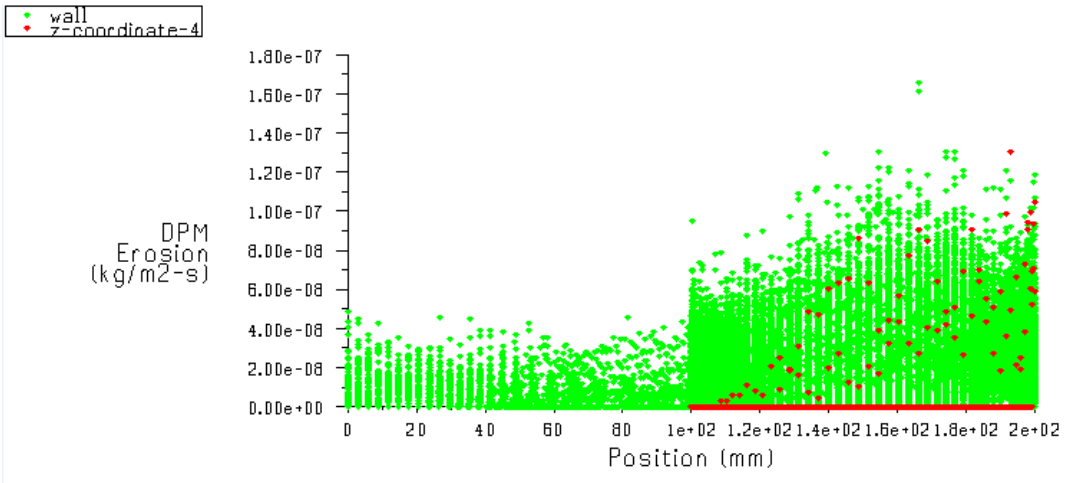

Figure 4.28: Magnitude and location of erosion at bend wall and outlet at velocity 2.5 m/s, concentration 10% and particle size 162 μm.

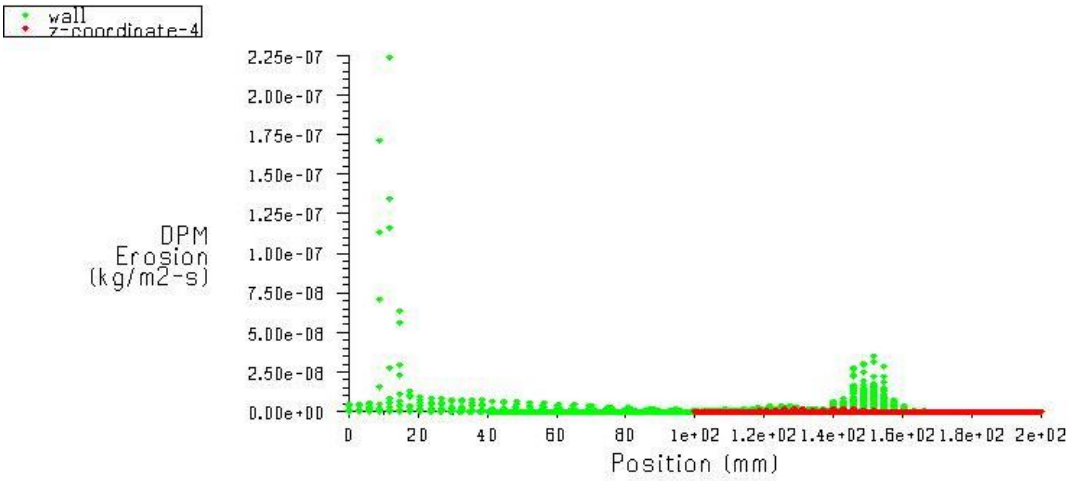

Figure 4.29: Magnitude and location of erosion at bend wall and outlet at velocity 0.5 m/s, concentration 10% and particle size 300 μm.

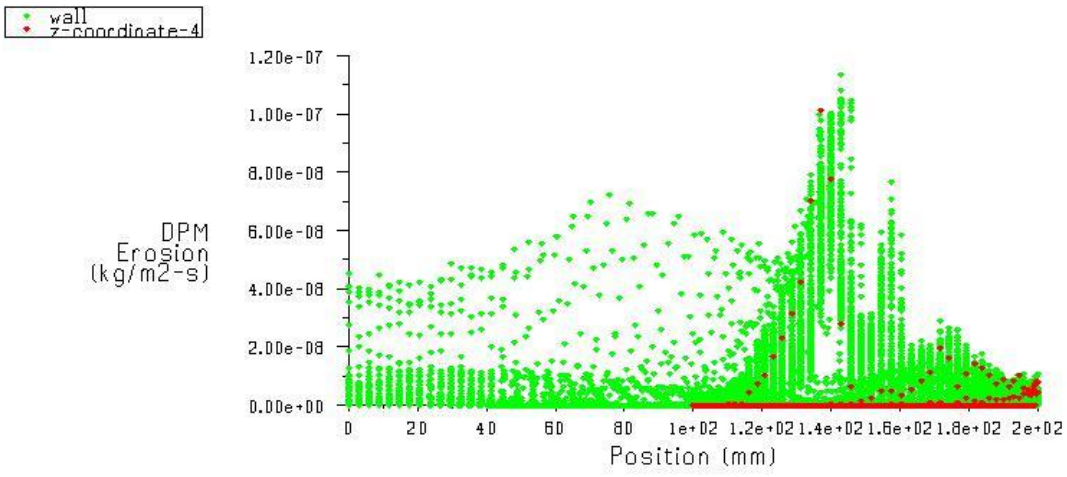

Figure 4.30: Magnitude and location of erosion at bend wall and outlet at velocity 1.5 m/s, concentration 10% and particle size 300 μm.

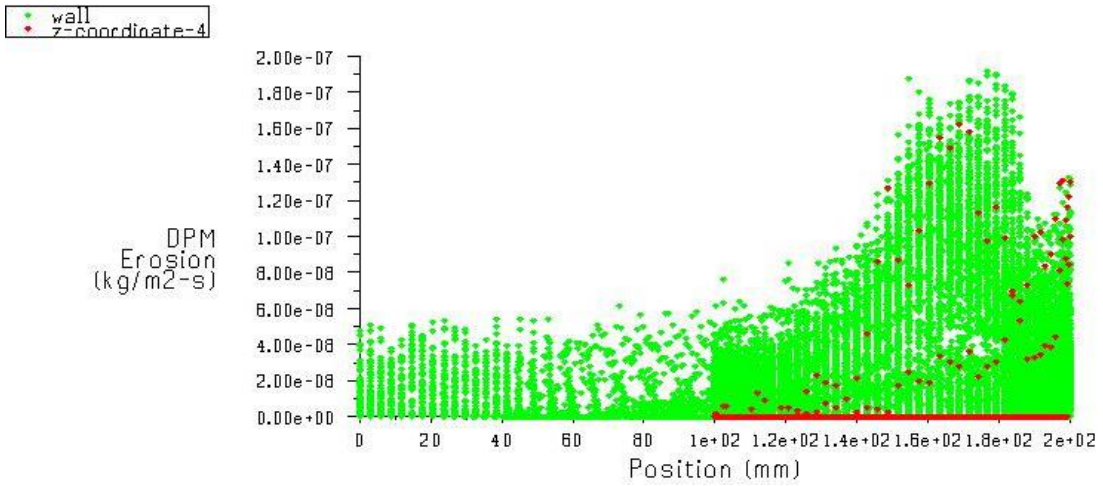

Figure 4.31: Magnitude and location of erosion at bend wall and outlet at velocity 2.5 m/s, concentration 10% and particle size 300 μm.

CHAPTER 5 CONCLUSIONS

5.1 CONCLUSIONS

Computation fluid dynamics code FLUENT was used analyze the slurry erosion in pipe bend for the flow bottom ash slurry. based on the results conclusions are given below:

- The erosion wear in the horizontal pipe bend is greatly influenced with velocity of the flowing medium.
- At low velocity settling takes place in the pipe bend due to low inertia and gravitational effect on the solid particulate, leads to erosion at bottom side of pipe line.
- Erosion wear takes place sever times more in curved sections than straight once.
- At high velocity erosion high magnitude shifts toward the outer side of the bend due to centrifugal action.
- Significant of the solid concentration is very less for the erosion wear.
- The erosion rate is also varies with the particles size along with velocity not much with solid concentration.

5.2 FUTURE SCOPE

The present study has been done to predict the erosion rate and effect of the solid concentration, velocity and particles size on the horizontal 90^{o} pipe-bend. So this work can also be continuing for the long radius bend and centrifugal slurry pump impeller –section by numerical simulation.

REFERENCES

[1]. Modi O.P., Dasgupta R., Prasad B.K., Jha A.K., Yegneswaran A.H. and Dixit G., (2000), "Erosion of a high-carbon Steel in Coal and Bottom-Ash Slurries", *Journal of Materials Engineering and Performance*, 9:522-529.

[2]. Zheng Z., Xuewen C. and Yugui Z., (2000), "Numerical Simulation of Erosion Corrosion in the Liquid Solid Two-Phase Flow", *Chinese Journal of Chemical Engineering*, 8(4):347-355.

[3]. Edwards J.K., McLaury B.S. and Shirazi S.A., (2001), "Modeling Solid Particle Erosion in Elbows and Plugged Tees", *Journal of Energy Resources Technology*, 123:277-284.

[4]. Bozzini B., Ricotti M.E., Boniardi M. and Mele C., (2003), "Evaluation of Erosion–Corrosion in Multiphase Flow via CFD and Experimental Analysis", *Wear*, 255:237-245.

[5]. Wood R.J.K. and Jones T.F., (2003), "Investigations of Sand–Water Induced Erosive Wear of AISI 304L Stainless Steel Pipes by Pilot-Scale and Laboratory-Scale Testing", *Wear*, 255:206-218.

[6]. Chen X., Mclaury B.S. and Shirazi S.A., (2004), "Application and Experimental Validation of a Computational Fluid Dynamics (CFD)-Based Erosion Prediction Model in Elbows and Plugged Tees", *Computer and Fluid*, 33:1251-1272.

[7]. Habib M.A., Badr H.M., Mansour R.B and Said S. A. M., (2004), "Numerical Calculations of Erosion in an Abrupt Pipe Contraction of Different Contraction Ratios", *International Journal for Numerical Methods in Fluids*, 46:19-35.

[8]. Wood R.J.K., Jones T.F., Ganeshalingam J. and Miles N.J., (2004), "Comparison of Predicted and Experimental Erosion Estimates in Slurry Ducts", *Wear*, Vol. 256:937–947.

[9]. Gnanavelu A., Kapur N., Neville A. and Flores J.F., (2009), "An Integrated Methodology for Predicting Material Wear Rates Due to Erosion", *Wear*, 267: 1935–1944.

[10]. Graham L.J.W, Lester D and Wu J., (2009), "Surry Erosion in Complex Flows: Experiment and CFD", *CSIR :*1-6.

[11]. Gnanavelu A., Kapur N., Neville A. and Flores J.F., (2011), "A numerical investigation of a geometry independent integrated method to predict erosion rates in slurry erosion", *Wear*, 271:712– 719.

[12]. Stack M.M. and Abdelrahman S.M. (2011) “A CFD model of particle concentration effects on erosion–corrosion of Fe in aqueous conditions”, *Wear*, 273:38– 42.

[13]. Mazumder Q.H., (2012), “Effect Of Liquid and Gas Velocities on Magnitude and Location af Maximum Erosion in U-Bend”, *Open Journal of Fluid Dynamics*, 2:29-34.

[14]. Njobuenwu D.O. and Fairweather M., (2012), “Modelling of Pipe Bend Erosion by Dilute Particle Suspensions", *Computers and Chemical Engineering*, 42: 235–247.

[15]. Okita R., Zhang Y., McLaury B.S. and Shirazi S.A. (2012), “Experimental and Computational Investigations to Evaluate the Effects of Fluid Viscosity and Particle Size on Erosion Damage”, *Journal of Fluids Engineering*, 134:061301-13.

[16]. Zhang H., Tan Y., Yang D., Trias F.X., Jiang S., Sheng Y., Oliva A., (2012), “Numerical investigation of the location of maximum erosive wear damage in elbow, Effect of slurry velocity, bend orientation and angle of elbow”, *Powder Technology*, 217:467–476.

[17]. Wu H., Liang X. and Deng Z. *(2013), “*Numerical simulation on typical parts erosion of the oil pressure pipeline”, *Thermal Science*, 17(5):1349-1353.

[18]. Fluent Theory Guide, 2015.

[19]. Hadziahmetovic H., Hodzic N., Kahrimanovic D. and Dzzaferovic E., (2014), “Computational Fluid Dynamics (Cfd) Based Erosion Prediction Model in Elbows”, *Tehnicki vjesnik*, 21(2): 275-282.

[20]. Kumar S., Gandhi B.K. and Mohapatra S.K., (2014), “Performance Characteristics of Centrifugal Slurry Pump with Multi-Sized Particulate Bottom and Fly Ash Mixtures”, *Particulate Science and Technology*, 32:466-476.

[21]. Mansouri A., Arabnejad H., Shirazi S.A. and McLaury B.S. (2014),” A combined CFD/experimental methodology for erosion prediction”, *Wear*:8

[22]. Pereira G.C., Souza F.J,D. and Souza D.A.D.M., (2014), “Numerical prediction of the erosion due to particles in elbows”, *Powder Technology*, 261:105–117

[23]. Safaei M. R. , Kazi S. N., Gharehkhani S., Mahian O., Garoosi F., and Hooman K., Karimipour A., (2014), “Investigation of Micro and Nanosized Particle Erosion in a 90^{O} Pipe Bend Using a Two-Phase Discrete Phase Model”, *The Scientific World Journal*, 2014:12.

[24]. Singh P.,(2014), “Investigation of Slurry erosion in Pipeline Materials”, M.E. Thesis of Thapar University Patiala :1-88.

[25]. Zeng L., Zhang G.A., Guo X.P., (2014), “Erosion–corrosion at different locations of X65 carbon steel elbow”, *Corrosion Science*:1-13.

[26]. Chen J., Wang Y., Li X., He R, Han S. and Chen Y., (2014), “Erosion prediction of liquid-particle two-phase flow in pipeline elbows via CFD–DEM coupling method”, *Powder Technology* 275:182–187.